Physics – Uspekhi **41** (11) 1091 – 1114 (1998)

REVIEWS OF TOPICAL PROBLEMS PACS numbers: **36.40.–c**, **61.46.+w**, **61.48.+c**

Fullerenes in solutions

V N Bezmel'nitsyn, A V Eletskiĭ, M V Okun'

Contents

1. Introduction **1091**
2. Solubility of fullerenes **1093**
2.1 Experimental data; 2.2 Temperature dependence of the solubility of fullerenes; 2.3 Cluster origin of the solubility of fullerenes; 2.4 Heat of solution of fullerene C_{60}
3. Transfer phenomena in fullerene solutions **1100**
3.1 Diffusion of fullerenes in solutions; 3.2 Thermal diffusion of fullerenes in solutions
4. Optical properties of fullerenes in solutions **1104**
4.1 Nonlinear optical susceptibility; 4.2 Solvatochromism
5. Fractal structures in fullerene solutions **1106**
5.1 Measurement of the kinetics of fractal structure growth using the light scattering methods; 5.2 The aggregation of particles in solutions. Diffusion approach; 5.3 Models of fractal cluster growth in fullerene solutions; 5.4 Small and large clusters in fullerene solutions
6. Thermodynamic parameters of fullerite **1109**
6.1 Close-packed crystals and short-range intermolecular interaction; 6.2 Binding energy of fullerenes in crystals; 6.3 Saturated vapor pressure; 6.4 Thermodynamic parameters of fullerite; 6.5 The problem of the existence of liquid fullerite
7. Conclusions **1112**
References **1113**

Abstract. Phenomena and processes related to the behavior of fullerenes in solutions are reviewed. Data on the solubility of C_{60} and C_{70} fullerenes in a large number of solvents at various temperatures are presented as well as on diffusion coefficient of fullerenes in solutions. The relation between the factors controlling the behavior of dissolved fullerenes and the clustering tendency they show is analyzed. This tendency, which sets fullerenes apart from other large molecules, underlies many aspects of fullerene behavior in solutions, such as the recently discovered nonmonotone temperature dependence of fullerene solubility in various solvents, the nonlinear concentration dependence of nonlinear optical susceptibility, the sharp dependence of the color of a fullerene solution on the solution composition (the solvatochromatic effect), the concentration dependence of the heat of solution of fullerenes in organic solvents, etc. Growth mechanisms of fractal clusters in fullerene solutions are analyzed along with similarity laws determining the thermodynamic characteristics of fullerite crystals.

1. Introduction

One of the most rapidly developing directions of contemporary chemical physics is associated with the discovery and study of fullerenes, which represent a novel allotrope of carbon [1 – 6]. Carbon atoms in fullerene molecules are located at the vertices of regular hexagons and pentagons, which cover in a regular manner the surface of a sphere or spheroid. The most spread and elaborated of molecules belonging to the fullerene family is C_{60}, whose structure is a regular truncated icosahedron. The surface of this molecule is constructed from twenty regular hexagons and twelve regular pentagons so that each pentagon is adjacent only to hexagons, whereas each hexagon is adjacent to three pentagons and three hexagons alternately. The fullerene family also includes along with C_{60} the molecules C_{70}, C_{76}, C_{78}, C_{84}, etc., distinguished by a lower symmetry and larger number of hexagons on the surface. Thus, the fullerenes form a unique class of molecules having a closed two-dimensional structure.

The interest in studying fullerenes rose considerably after the development of the technology for their synthesis in macroscopic (gram) quantities [2, 3]. This interest has two main reasons. Firstly, fullerenes as a new object of chemical physics are characterized by unusual properties, which are displayed in various conditions. Between these properties should be mentioned primarily the geometry of the molecule itself, the peculiar crystal structure of solid fullerenes which can be drastically changed as a result of relatively small variations in the temperature and pressure, as well as their extraordinary behavior in solutions and chemical processes. Secondly, the fullerenes are of considerable interest for applications as a novel material having wide prospects for scientific and technological purposes. Noteworthy are a new class of superhard materials produced recently on the base of fullerenes; superconducting compounds of fullerenes with alkali and alkali-earth metals; thin films and fullerene

V N Bezmel'nitsyn, A V Eletskiĭ, M V Okun'
Russian Research Center 'Kurchatov Institute'
Kurchatov Square 1, 123182 Moscow, Russia
Tel. (7-095) 196-72 80
E-mail: eletskii@imp.kiae.ru

Received 17 February 1998, revised 6 April 1998
Uspekhi Fizicheskikh Nauk **168** (11) 1195 – 1220 (1998)
Translated by A V Eletskiĭ; edited by A Radzig

solutions, having nonlinear optical properties; various fullerene-based compounds and polymers, having unique physical, chemical and mechanical characteristics. A detailed review of the present state of the art of research and development in the field of fullerenes can be found particularly in Refs [5, 6].

The interest in studying the behavior of fullerenes in solutions is twofold. It has both basic and applied aspects. The basic interest in this problem is mainly motivated by the fact that the fullerene is the only one of the three presently known allotropic form of carbon (graphite, diamond, fullerenes) which exhibits a marked solubility in organic solvents of a wide class. Such a peculiarity is due to the extraordinary structure of fullerenes, which as distinct from other carbon modifications has no sharp ridges and dangling bonds characterized by an enhanced chemical reactivity. This determines the relatively weak interaction of fullerene molecules inside a crystal with one another and, in turn, promotes the dissolution of fullerene molecules in organic solvents whose molecular structure contains aromatic six-membered carbon rings similar in form to elements of the surface structure of fullerenes.

The exotic structure of fullerenes also determines their extraordinary behavior in solutions. Since the specific surface energies of interaction of fullerene molecules with one another and with solvent molecules are close in magnitude, fullerenes in solutions display a trend to the formation of aggregates or clusters consisting of a number of molecules. In a quite highly concentrated solution in the state of thermodynamic equilibrium, the overwhelming majority of dissolved substance is in the cluster form. To the best of the author's knowledge, this is the only example of a situation, when essentially the whole of substance is in 'cluster' state. The situation, when the portion of substance involved in clusters is relatively low, seems as more typical. Thus, the study of the behavior of fullerenes in solutions not only provides new information on fullerene properties, but also extends our notions about macroscopic characteristics of a substance consisting mainly of clusters.

Extraordinary physical and chemical peculiarities in the behavior of fullerenes in solutions are related on the one hand to their exotic structure and on the other hand to the possibility of cluster formation. This makes fullerene solutions an interesting object of chemical physics, possessing unusual thermodynamic, kinetic, optical and other properties. Among these unusual properties should be mentioned the recently discovered nonmonotone temperature dependence of solubility of fullerenes in some solvents [7] as well as the nonlinear concentration dependence of the third-order nonlinear optical susceptibility [8]. Of considerable scientific interest is the observed recently solvatochromatic effect [9, 10], which is exhibited in a sharp alteration in the spectrum of the optical absorption of C_{70}, dissolved in a mixture of organic solvents, as a result of a slight change in the solvent content. These and some other peculiarities in the behavior of fullerenes in solutions are attributable to the phenomenon recently predicted theoretically [11, 12] and revealed in experiments [13 – 15] of the formation of clusters (consisting of a number of fullerene molecules) in a solution. A thermodynamic approach to the description of this phenomenon based on a droplet model of a cluster [11, 12, 16] enables one to uniquely describe numerous peculiarities in the behavior of fullerenes in solutions and on this basis to predict new effects such as the concentration and temperature dependences of the diffusion and thermal diffusion coefficients of fullerenes in solutions as well as the concentration dependence of the heat of solution of fullerenes.

Another reason for an enhanced interest in the study of the behavior of fullerenes in solutions lays in the existing methods for production and purification of fullerenes in macroscopic quantities, which are based on the use of solvents [2, 3]. As a result of intense thermal action on a crystal graphite surface a soot is formed, containing up to 20% fullerenes. The most convenient method for thermal action is based on the use of an arc discharge between graphite electrodes in an atmosphere of a buffer gas which is usually helium.

The fullerenes are separated from the soot due to their capacity, unlike other components of soot, to dissolve quite well in organic and some other solvents (toluene, benzene, xylene, CS_2, etc.). The most generally employed technology of further separation of fullerenes of different sorts and their subsequent purification is based on the concept of liquid chromatography [3, 17]. A fullerene solution is passed under pressure through a sorbent whose sorption properties are characterized by marked differences with respect to fullerene molecules of different sizes. Fullerene molecules are sorbed on the surface of a porous sorbent such as carbon black, silica gel, or alumina. The subsequent flow of a pure solvent through the sorbent filled with fullerene molecules results in washing out these molecules. In view of the differences in the sorption capacity of the sorbent with respect to fullerene molecules, the washing out of fullerene molecules of different types occurs successively, so that at each moment of time fullerene molecules of a certain mass predominate in the given unit volume of solvent. The efficiency of the above-described technology of separation and purification of fullerenes depends both on the sorbent properties and on features in behavior of fullerene molecules in the solvent.

Another generally employed method for separation and purification of fullerenes is based on the phenomenon of fullerene crystallization in solutions [18, 19]. The evaporation of solvent from a solution containing fullerenes of different sorts with drastically different concentrations causes the crystallization of fullerenes of the sort whose concentration is maximum and close to saturation. This provides the production of crystals involving predominantly the fullerene molecules of a certain sort.

Obviously, in order to fully realize all of the capabilities of the above-described methods of preparation, separation, and purification of fullerenes, one needs both a profound understanding of the peculiarities of their behavior in solutions and the knowledge of important parameters such as the solubility, diffusion and thermal diffusion coefficients, etc., which determine this behavior. The results of measuring the above-identified parameters are given in this review.

In this article a wide class of phenomena accompanying the behavior of fullerenes in solutions is reviewed from a unique point of view, taking into account the tendency of fullerenes to cluster formation in solutions. The available experimental data are given concerning the solubility of fullerenes C_{60} and C_{70} in a variety of solvents at various temperatures as well as the diffusion coefficient of fullerenes in solutions. Experiments revealing extraordinary peculiarities in the behavior of fullerenes in solutions are analyzed. Those peculiarities are considered on the basis of a droplet model of cluster, in which frames it is performed a consistent thermodynamic description of the behavior of fullerenes in

solutions. This provides a quantitative examination for observed unusual thermodynamic and optical characteristics of fullerene solutions and the prediction of new effects in the solutions of fullerenes in organic solvents such as concentration and temperature dependences for diffusion and thermal diffusion coefficients, as well as concentration dependence for the heat of solution. Based on modern approaches to the description of mechanisms of fractal cluster growth, the recently performed experiments concerning the kinetics of fractal cluster formation in fullerene solutions are considered. Similarity laws determining the thermodynamic properties of fullerite crystals which are characterized by the close-packed, face-centered cubic structure and short-range intermolecular interaction are analyzed. In this review, the data contained in the recent review article of one of the authors are partly used [20].

2. Solubility of fullerenes

2.1 Experimental data

As already mentioned in the Introduction, the possibility of effective extraction of fullerenes from fullerene-containing soot formed as a result of thermal sputtering of graphite is due to the relatively high (as compared with other components of soot) solubility of fullerenes in numerous organic solvents. The most efficient method of separation of fullerenes is based on the differences in the solubility of different fullerenes in a number of solvents, as well as on the differences in the effectiveness of their washing out from sorbents with the aid of a solvent. Due to those differences, the extraction of various fullerenes from sorbents using solvent is characterized by varied effectiveness. Therewith, at a proper choice of a sorbent – solvent pair the time delay in the extraction of different kinds of fullerene molecules can reach tens of minutes. The principles underlying the most efficient methods of separation and purification of fullerenes are analogous to those which lie at the basis of liquid chromatography.

Tables 1 – 3 give the results of measurements of the solubility of fullerenes at room temperature in a number of solvents. (Many of these data are summarized in the review article [21]). As seen from the tabular data, the solubility of fullerenes of different sorts (C_{60} and C_{70}) are of the same

Table 1. Solubility of fullerene C_{60} at room temperature.

Solvent	Solubility, mg ml^{-1}
***Nonaromatic hydrocarbons*:**	
Noncyclic:	
n-pentane	0.005 [22]; 0.004 (303 K) [23]
n-hexane	0.043 [22]; 0.040 (303 K) [23]; 0.052 [7]
octane	0.025 (303 K) [23]
isooctane	0.026 (303 K) [23]
n-decane	0.071 [22]; 0.070 (303 K) [23]
dodecane	0.091 (303 K) [23]
tetradecane	0.126 (303 K) [23]
Cyclic:	
cyclopentane	0.002 [23]
cyclohexane	0.036 [22]; 0.035 [24]; 0.051 (303 K) [23]
decalin (3:7 *cis* and *trans* mixture)	4.60 [22]
cis-decalin	2.20 [22]
trans-decalin	1.30 [22]
1, 5, 9-cyclododecatrien	7.14 [25]

Table 1 (*Continued*)

Solvent	Solubility, mg ml^{-1}
Cyclic derivatives:	
cyclopentyl bromide	0.41 [24]
cyclohexyl chloride	0.53 [24]
cyclohexyl bromide	2.20 [24]
cyclohexyl iodide	8.06 [24]
(+ –)-*trans*-1, 2-dibromocyclohexane	14.28 [25]
cyclohexane	1.21 [25]
1-methyl-1-cyclohexane	1.03 [25]
methylcyclohexane	0.17 [25]
1, 2-dimethylcyclohexane (*cis* and *trans* mixture)	0.13 [25]
ethylcyclohexane	0.25 [25]
Halogen-containing alkanes:	
dichloromethane	0.26 [22]; 0.23 [24]; 0.25 (303 K) [23]
tetrachloromethane	0.32 [22]; 0.45 [26]
chloroform	0.16 [22]; 0.17 [25]; 0.25 [26]
carbon tetrachloride	0.32 [22]; 0.45 (303 K) [23]
dichloroethane	0.36 [24]
bromoform	5.64 [24]
iodomethane	0.13 [24]
bromochloromethane	0.75 [25]
bromoethane	0.07 [25]
iodoethane	0.28 [25]
Freon TF (dichlorodifluoroethane)	0.02 [22]
1, 1, 2-trichlorotrifluoroethane	0.01 [22]
1, 1, 2, 2-tetrachloroethane	5.30 [22]
1, 2-dichloroethane	0.08 [24]
1, 2-dichloromethane	0.50 [22]
1, 1, 1-trichloroethane	0.15 [24]
1-chloropropane	0.02 [25]
1-bromopropane	0.05 [24]
1-iodopropane	0.17 [24]
2-chloropropane	0.01 [25]
2-bromopropane	0.03 [25]
2-iodopropane	0.11 [24]
1, 2-dichloropropane	0.10 [24]
1, 3-dichloropropane	0.12 [24]
(+ –)–1, 2-dibromopropane	0.35 [24]
1, 3-dibromopropane	0.40 [25]
1, 3-diiodopropane	2.77 [24]
1, 2, 3-trichloropropane	0.64 [24]
1, 2, 3-tribromopropane	8.31 [24]
1-chloro-2-methylpropane	0.03 [24]
1-bromo-2-methylpropane	0.09 [25]
1-iodo-2-methylpropane	0.34 [24]
2-chloro-2-methylpropane	0.01 [25]
2-bromo-2-methylpropane	0.06 [25]
2-iodo-2-methylpropane	0.23 [25]
1, 2-dibromoethylene	1.84 [24]
trichloroethylene	1.40 [22]
tetrachloroethylene	1.20 [22]
1-chloro-2-methylpropane	0.21 [25]
Halogen-containing alkynes:	
bromopropin	0.22 [25]
***Aromatic hydrocarbons*:**	
benzene	1.70 [22]; 1.50 [27]; 0.88 [25]; 0.89 [28]; 1.44 (303 K) [23]
Benzene derivatives:	
toluene	2.80 [22]; 2.90 [27]; 0.54 [27]; 2.90 [29]; 2.15 (303 K) [23]
1, 2-dimethylbenzene	8.70 [27]; 7.35 [24]; 9.30 [29]
1, 3-dimethylbenzene	1.40 [27]; 2.83 [24]
1, 4-dimethylbenzene	5.90 [27]; 3.14 [24]
1, 2, 3-trimethylbenzene	4.70 [27]
1, 2, 4-trimethylbenzene	17.90 [27]
1, 3, 5-trimethylbenzene	1.50 [22]; 1.70 [27]; 1.00 (303 K) [27]
1, 2, 3, 4-tetramethylbenzene	5.80 [27]

Table 1 (*Continued*)

Solvent	Solubility mg ml^{-1}
1, 2, 3, 5-tetramethylbenzene	20.80 [27]
ethylbenzene	2.60 [27]; 2.16 [24]
n-propylbenzene	1.50 [27]
isopropylbenzene	1.20 [27]
n-butylbenzene	1.90 [27]
hexabutylbenzene	1.10 [27]
tributylbenzene	0.90 [27]
tetrahydronaphthalene	16.00 [22]
Halogen derivatives:	
fluorobenzene	0.59 [22]; 1.20 [27]
chlorobenzene	7.00 [22]; 5.70 [27]
bromobenzene	3.30 [22]; 2.80 [27]
iodobenzene	2.10 [27]
1, 2-dichlorobenzene	27.00 [22]; 24.60 [27]; 7.11 [30]
1, 2-dibromobenzene	13.80 [27]
1, 3-dichlorobenzene	2.40 [27]
1, 3-dibromobenzene	13.80 [27]
1, 2, 4-trichlorobenzene	8.50 [22]; 10.40 [27]; 4.85 [30]
Other derivatives:	
o-creosol	0.01 [22]
benzonitrile	0.41 [22]
nitrobenzene	0.80 [22]
methoxybenzene	5.60 [22]
benzaldehyde	0.42 [24]
pentylisooctane	2.44 [24]
2-nitrotoluene	2.43 [24]
3-nitrotoluene	2.36 [24]
thiophenol	6.91 [25]
Benzyl derivatives:	
benzylchloride	2.46 [24]
benzylbromide	4.94 [24]
α, α, α-trichlorotoluene	4.80 [24]
Naphthalene derivatives:	
1-methylnaphthalene	33.00 [22]; 33.20 [27]
dimethylnaphthalene	36.00 [22]
1-phenylnaphthalene	50.00 [22]
1-chloronaphthalene	51.00 [22]
1-bromo-2-methylnaphthalene	34.80 [27]
***Polar solvents*:**	
methanol	0.000 [27]; 0.000035 [31]
ethanol	0.001 [22]; 0.0008 [31]
1-propanol	0.0041 [31]
1-butanol	0.094 [31]
1-pentanol	0.030 [31]
1-hexanol	0.042 [31]
1-octanol	0.047 [31]
nitromethane	0.000 [22]
nitroethane	0.002 [22]
acetone	0.001 [22]
acetonitrile	0.000 [22]
acrylonitrile	0.0040 [25]
n-butylamine	3.688 [30]
monomethylglycol ether	0.032 [24]
N, N-dimethylformamide	0.027
dioxane	0.041 (303 K) [23]
***Miscellaneous*:**	
CS_2	7.90 [22]; 7.70 [29]; 7.90 [23]; 5.16 (303 K) [23]
tetrahydrofuran	0.00 [22]; 0.06 [30]
thiophene	0.40 [27]; 0.24 [30]
tetrahydrothiophene	0.03 [22]; 0.11 [30]
2-methylthiophene	6.80 [22]
N-methyl-2-pyrrolidone	0.89 [22]
pyridine	0.89 [22]; 0.30 [27]
methithilol	1.5 [22]; 1.0 [26]
quinoline	7.20 [27]
***Inorganic solvents*:**	
water	1.3×10^{-11} [31]
silicon (IV) chloride	0.09 [25]
germanium (IV) chloride	0.50 [25]
hexachlorodisilan	0.38 [25]
silicon (IV) bromide	0.74 (305 K) [25]
germanium (IV) bromide	0.68 (305 K) [25]
tin (IV) bromide	0.17 (305 K) [25]

Table 1 (*Concluded*)

Table 2. Solubility of fullerene C_{70} at room temperature.

Solvent	Solubility, mg ml^{-1}
n-penthane	0.002 [26]
n-hexane	0.013 [26]
n-decane	0.053 [26]
dodecane	0.098 [26]
dichloromethane	0.08 [26]
tetrachloromethane	0.12 [26]
isopropanol	0.0021 [26]
acetone	0.0019 [26]
benzene	1.3 [26]
toluene	1.4 [26]
xylene	14.3 [29]
methithilol	1.47 [26]
1, 2-dichlorobenzene	36.2 [26]
carbon disulfide (CS_2)	9.9 [26]

order, however, these quantities can differ from one another as much as several times. This difference makes up the basis for one of the most effective methods for separation of fullerenes. Fullerenes are almost insoluble in polar solvents such as alcohols, in acetone, tetrahydrofurane, etc. They are weakly soluble in alkanes of normal structure (pentane, hexane, and decane); their solubility in alkanes increases with the number of carbon atoms. As revealed by the analysis performed by the authors of Ref. [22], fullerenes are best dissolved in solvents for which the value of specific enthalpy of vaporization, referred to the volume of solvent molecule, is close to the corresponding value for a molecule of C_{60} (approximately 100 cal cm^{-3}). This peculiarity can be regarded as a possible quantitative manifestation of the old empirical rule 'like dissolves in like'. The complicated behavior of fullerenes in solutions shows up, in particular, in the data on the solubility of C_{60} in decalin. As follows from these measurements, the solubility of fullerenes in normal decalin consisting of a 3:7 mixture of the *cis*- and *trans*- forms appreciably exceeds the respective values for each form separately.

The data presented in Tables 1 – 3 permit formulation of some general regularities which might help to illuminate the nature of the solubility of fullerenes in one or another type of solvents. First of all it should be noted the extraordinary low solubility of fullerenes in polar solvents. This points to unessential role of the solvation mechanism of solution, involving the formation of long-lived complexes (solvates), i.e. the solute molecule surrounded by a shell of correspondingly oriented molecules of a solvent. The most high solubility of fullerenes is shown by aromatic hydrocarbons and their derivatives, the first positions in the list occupied by naphthalene derivatives. Since aromatic compounds are built on the basis of one or several benzene rings, whose structure is close to that of regular hexagons inherent to fullerene surfaces, this feature is hardly occasional. It might be supposed that the high solubility of fullerenes in com-

Table 3. Solubility of fullerene C_{60} at different temperatures.

Solvent	T, (K)	Solubility	
		mg ml^{-1}	molar fraction, 10^4
n-hexane	195		0.011 [7]
	238		0.03 [7]
	273		0.07 [7]
	283		0.12 [7]
	288		0.10 [7]
	298		0.09 [7]
	318		0.07 [7]
	338		0.07 [7]
	338.1		1.80 [28]
toluene	298.1		0.80 [28]
	308.1		0.90 [28]
	328.1		1.20 [28]
	338.1		1.50 [28]
	233	0.75 [29]	
	243	0.96 [29]	
	248	1.30 [29]	
	253	1.50 [29]	
	258	1.90 [29]	
	263	2.50 [29]	
	268	3.20 [29]	
	273	4.00 [29]	
	278	3.90 [29]	
	283	3.70 [29]	
	293	3.30 [29]	
	298	2.90 [29]	
	303	2.70 [29]	
	313	2.30 [29]	
	323	2.20 [29]	
	333	1.90 [29]	
	343	1.80 [29]	
	353	1.50 [29]	
	195		0.14 [7]
	253		1.93 [7]
	258		2.79 [7]
	273		4.79 [7]
	278		4.93 [7]
	283		3.79 [7]
	288		3.93 [7]
	295		4.21 [7]
	298		4.07 [7]
	313		3.29 [7]
	353		1.57 [7]
	383		1.29 [7]
1, 2-dimethylbenzene	253	1.60 [29]	
	263	2.50 [29]	
	273	3.50 [29]	
	283	5.00 [29]	
	288	6.20 [29]	
	293	7.70 [29]	
	298	9.30 [29]	
	300.5	10.20 [29]	
	303	10.30 [29]	
	305.5	9.30 [29]	
	308	8.40 [29]	
	313	7.40 [29]	
	323	6.10 [29]	
	333	5.30 [29]	
	343	4.90 [29]	
	353	4.40 [29]	
1, 2-dichlorobenzene	298.1		11.10 [30]
	308.1		13.40 [30]
	318.1		15.10 [30]
	328.1		17.80 [30]

pounds, whose structure includes six-membered carbon rings, is caused by the magnetic interaction between the ring current in a solvent molecule and that in a fullerene molecule. The specific surface energy for such an interaction is of the same order of magnitude as the interaction energy of adjacent fullerene molecules in a crystal. For this reason, the heat of solution of fullerenes is rather low. The magnetic field caused by the intramolecular current in a six-membered fullerene ring aligns an aromatic compound molecule in such a manner that the inner current of this molecule is directed opposite to that in a fullerene ring. The energy of magnetic interaction of these currents determines the positive thermal effect of dissolving fullerene molecules.

2.2 Temperature dependence of the solubility of fullerenes

One of the most striking peculiarities in the behavior of fullerenes in solutions relates to an extraordinary temperature dependence of their solubility. This dependence was originally discovered in the experiment [7], where the solubility of C_{60} in hexane, toluene and CS_2 was measured in the temperature range 200–400 K. The results of these measurements are presented in Fig. 1. The data are supplemented with the temperature dependence of the solubility of C_{60} in xylene, measured in Ref. [29]. As seen from these data, whereas the absolute values of the solubility of C_{60} for different solvents differ over two orders of magnitude, the temperature dependence of the solubility is almost independent of the type of solvent over a wide range of temperature variation. Further, our attention is engaged by the experimentally established nonmonotone behavior of the temperature dependence of the solubility of fullerenes. This dependence reaches its maximum magnitude near 280 K and notably decreases at further enhancement of temperature. It is of interest to note that the nonmonotone temperature dependence of solubility is inherent only to C_{60} and not observed for fullerenes of other sorts. Thus, in Fig. 2 the temperature dependences of the solubility of fullerene C_{70} in

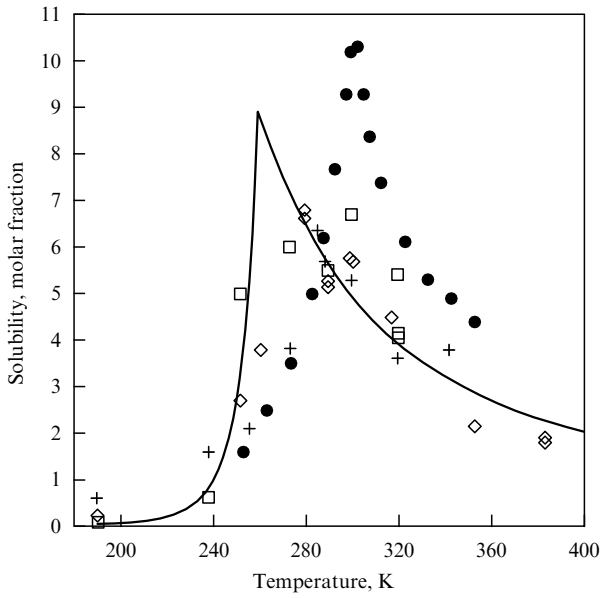

Рис. 1. Temperature dependence of the solubility of fullerene C_{60}: + — in hexane (times 55); □ — in toluene (times 1.4); ◇ — in CS_2; • — in xylene. The solid line shows the results of calculations using the droplet madel.

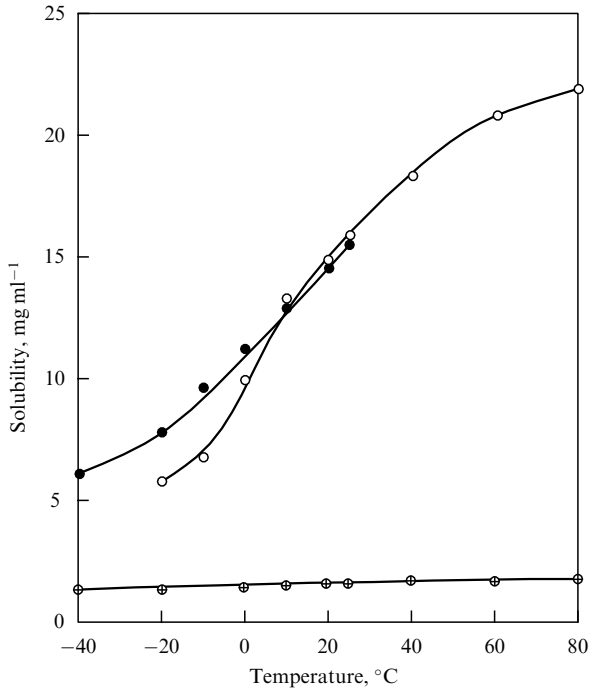

Рис. 2. Temperature dependence of the solubility of fullerene C_{70} in toluene (⊕), xylene (○) and CS_2 (●).

toluene, xylene and CS_2 are given, measured in a recent publication [29]. As is seen, there is a monotonically rising temperature dependence, which is inherent to the majority of solvent — solute pairs. This basic distinction in temperature dependences of solubility of molecules close in structure shows the complicated nature of the phenomenon of solubility of fullerenes and, in particular, the possibility of existence of several various competing mechanisms of solubility of fullerenes. It may be supposed that for fullerenes of different sorts the different mechanisms of solubility prevail, which in turn are reflected in the shape of the temperature dependence at hand.

2.3 Cluster origin of the solubility of fullerenes

One of the mechanisms of solubility, which may explain the experimentally found distinctions in the temperature dependence of solubility of fullerenes of different sorts, is based on the possibility of formation in solution of clusters consisting of a number of fullerene molecules [11]. This aggregation phenomenon changes the thermodynamic parameters of fullerenes in solutions (free energy, chemical potential, etc.), which displays, naturally, the phase equilibrium and changes the magnitude of solubility. Thus, the observed lowering in the solubility of C_{60} with rising in temperature can be treated as a result of the thermal decomposition of clusters, which is accompanied with an increase in the interaction energy of fullerene molecules and solvent molecules and, correspondingly, with a displacement of the equilibrium toward the solid phase.

The thermodynamic approach to the description of the phenomenon of solubility of fullerenes, taking account cluster formation, is developed in Refs [11, 12, 16]. This approach is based on the droplet model of clusters, which is valid under conditions when the characteristic number of fullerene molecules in the cluster is $n \gg 1$. As follows from the analysis of experimental data, this requirement is satisfied quite well in the conditions where the nonmonotone dependence of solubility of fullerenes occurs.

Let us formulate the problem of determining the temperature dependence of solubility of fullerenes in terms of the possibility of forming clusters consisting of several fullerene molecules. In accordance with the general principles of thermodynamics, in a saturated solution of fullerenes the magnitudes of the chemical potential per fullerene molecule for dissolved substance and for a crystal, which is in equilibrium with solution, are equal. This equality is valid not only for isolated molecules in a solution, but also for clusters consisting of several fullerene molecules. According to the droplet model of clusters, the free energy of a cluster in a solution is made up of two parts, namely, the volume part, whose magnitude is proportional to the number of molecules n in the cluster, and the surface part proportional to $n^{2/3}$ [32, 33]. This corresponds to the assumption that clusters consisting of $n \gg 1$ particles have a spherical droplet shape and permit the Gibbs energy G_n for a cluster of size n to be represented as the sum

$$G_n = G_1 n - G_2 n^{2/3}\,, \tag{1}$$

where the parameters G_1 and G_2 are responsible for the contribution to the Gibbs energy of molecules placed inside the volume and on the surface of a cluster, correspondingly. The chemical potential μ_n of a cluster of size n in a solution is expressed through the equation

$$\mu_n = G_n + T \ln C_n\,, \tag{2}$$

where T is the temperature. Having regard to the equation (1), this results in

$$\mu_n = G_1 n - G_2 n^{2/3} + T \ln C_n\,, \tag{3}$$

where the parameters G_1 and G_2 are expressed in temperature units.

In a saturated solution of fullerenes, the cluster size distribution function is determined through the equilibrium condition linking the clusters of a specified size with a solid phase. This corresponds to the equality between the magnitudes of the chemical potential (per molecule) for molecules incorporated into clusters of any size and into crystal. This results in the following expression for the cluster size distribution function in a saturated solution:

$$f(n) = g_n \exp\left(\frac{-An + Bn^{2/3}}{T}\right), \tag{4}$$

where the parameter A is the equilibrium difference between the energies of interaction of a fullerene molecule with its surroundings in the solid phase and in the cluster volume; B is the similar difference for fullerene molecules located on the cluster surface; g_n is the statistical weight of a cluster of size n, which can depend, generally speaking, on both temperature and cluster size n. However, as is usually assumed, we will further neglect these dependences in comparison with the much stronger exponential dependence in Eqn (4). The presented form (4) for the cluster size distribution function is based on the structural features of fullerene molecules. In essence, a fullerene is a homogeneous surface structure which, unlike planar or elongated molecules, interacts with its

surroundings almost irrespective of orientation. The large number of similar elements of the fullerene surface makes it possible to represent the interaction energy of this molecule and the solvent molecules having essentially smaller size as the product of a specific surface interaction energy by surface area of the molecule. This feature of the fullerene structure may be further used in description of the interaction between clusters, made up of fullerenes, and the solvent. This is purely surface interaction and, because the interaction energy of fullerenes with one another both in a cluster and in a solid is low in comparison with the binding energy of carbon atoms in a fullerene molecule, one can assume that the specific surface energy of interaction of fullerene molecules with one another and with solvent molecules is not very sensitive to the relative orientation of fullerene molecules in a cluster.

Broadly speaking, the parameters A and B may have any sign. However, the normalization condition for the distribution function (4), having the obvious form

$$\sum_{n=1}^{\infty} f(n)n = C\,, \tag{5}$$

causes the requirement $A > 0$. Here C is the solubility expressed in relative units. In view of the condition $n \gg 1$, the normalization relationship (5) may be replaced by the integral

$$C = \bar{g}_n \int_{n=1}^{\infty} n \exp\left(\frac{-An + Bn^{2/3}}{T}\right) \mathrm{d}n\,. \tag{6}$$

Here $\bar{g}_n$ is the statistical weight of a cluster, averaged over the range of values of n that makes the major contribution to integral (6). This parameter includes the entropy factor and governs the absolute value of solubility and, generally speaking, may depend on the type of solvent.

Now let us analyze the possibility of using expressions (4)–(6) to describe the temperature dependences of solubility of fullerenes in nonpolar solvents, observed in Ref. [7] and plotted in Fig. 1. It is easy to verify that the contribution of clusters to those expressions can be notable only under condition of $B > 0$ [11]. In fact, calculating the first and the second derivative of integral (6) with respect to temperature, we can see that a nonmonotone temperature dependence of solubility arises under the conditions $A > 0$, $B > 0$, so that this dependence has one extremum (minimum) in which the second derivative of the solubility with respect to temperature is positive. Thus it turns out that the inclusion of the possibility of forming fullerene clusters is insufficient for the description of the experimentally found nonmonotone temperature dependence of the solubility of fullerenes, which has the maximum in the temperature range 260–280 K.

The numerical values of the parameters A and B, determining the energy of interaction of fullerene molecules with one another and with the solvent in a cluster and in a crystal, can be found through the comparison of the temperature dependence of solubility of fullerenes in some organic solvents, calculated using the droplet model, with experimental data. Generally speaking, the magnitudes of parameters A and B depend on the sort of solvent. However, considering the similarity in the temperature dependences of solubility in hexane, toluene and CS_2, observed in Ref. [7], the magnitudes of these parameters for indicated solvents may be thought as close to one another. The numerical fitting of the temperature dependence of the solubility of fullerenes, calculated using expression (6), to the experimental data [7] given in Fig. 1 and related to the drooping part of the dependence results in the following magnitudes: $A = 320$ K, $B = 970$ K for the temperature range above the point of orientation disorder phase transition in C_{60} crystal ($T_c \approx 260$ K).

For description of the growing part of the temperature dependence of the fullerene solubility in the low-temperature range ($T < T_c$) one needs to consider the orientation disorder phase transition, which takes place in C_{60} crystal at $T \approx 260$ K [34, 35]. As a result of this transition, a simple cubic lattice (sc) in the low-temperature C_{60} crystal is replaced by a face-centered cubic lattice (fcc) characterized by close packing. Further, the phase transition is accompanied by 'unfreezing' of the rotation of fullerene molecules around their axes. As shown by experiments [34, 35], it is an endothermic first-order phase transition, which is characterized by a heat of transition $\Delta h = 850$ K. The change in the Gibbs energy for the solid phase, produced by this phase transition, causes the corresponding change in the value of the parameter A determining the shape of the cluster size distribution function (4). In turn, this drastically changes the form of the distribution function and consequently is reflected in the form of the temperature dependence of the solubility of fullerenes in the temperature range below and above the critical point. Indeed, for $T < T_c$, the parameter

$$A_{sc} = A_{fcc} + \Delta h\,, \tag{7}$$

where A_{sc} and A_{fcc} are the values of the parameter A at temperatures above (simple cube) and below (face-centered cube) the critical temperature for phase transition. The higher magnitude of the A parameter in the low-temperature range ($T < T_c$) means that the cluster size distribution function (4) in this range drops with the number n much more sharply than in the case of $T > T_c$. The maximum of this function at low temperatures corresponds to the values of $n \approx 1$, so that the contribution of clusters to the solution behavior at $T < T_c$ is of little significance. This provides a qualitative explanation of the rising temperature dependence of solubility of fullerenes for $T < T_c$.

The temperature dependence of solubility of C_{60} in the low-temperature range was calculated in Refs [11, 12, 16] using the cluster size distribution function (4) and the magnitude of the parameter A changed according to the expression (6). The dependence thus obtained, tailored with that calculated previously for the high-temperature range, is compared in Fig. 1 with experimental data [7]. As is seen, a quite good fitting of the measured and calculated dependences $C(T)$ in the low-temperature range is reached using only the exact relation (7) without any additional suggestions concerning the magnitudes of parameters A and B. Some difference between the temperature at which the maximum magnitude of solubility is reached (~ 270 K) and the phase transition point $T_c \approx 260$ K may be attributed to the phase transition not really occuring at a single point, but over some quite broad temperature range $\Delta T \approx 20-40$ K [34, 35]. In this transition temperature range there is phase coexistence, which was not considered in the performance of the calculations described above.

The validity of the droplet model of clusters, used in this approach, is defined by the average number $\bar{n}$ of fullerene molecules per cluster. Figure 3 shows the distribution function of clusters over the size n, calculated at various

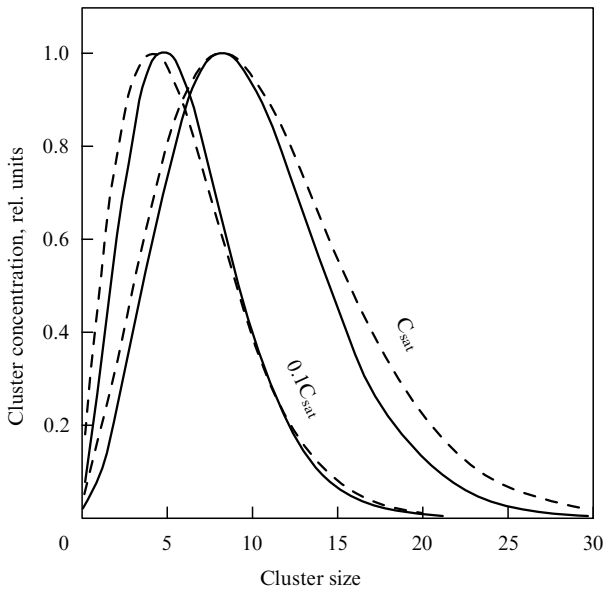

Рис. 3. Cluster distribution function by size in a solution of fullerene C_{60} in CS_2, calculated using the droplet cluster model for different concentrations at solvent temperatures $T = 280$ K (—) and 380 K (- - -).

temperatures for the saturated solution of C_{60} in CS_2 based on expression (4) and using the magnitudes of parameters A and B given above. As is seen from the data presented, the value of the parameter increases monotonically with temperature, from $\bar{n} = 3$ at $T = 190$ K to $\bar{n} = 11$ at $T = 260$ K. A further increase in the temperature up to 380 K has almost no effect on the value of $\bar{n}$. Therefore, in the temperature range corresponding to the maximum solubility of fullerenes, the condition $n \gg 1$ is valid, which supports the use of the droplet model and confirms the above-formulated assumption about the effect of the aggregation on the temperature dependence of solubility of fullerenes.

In such a manner the assumption about the cluster origin of the solubility of fullerenes, which follows from analysis of the experimental data [7–9, 13, 14, 22, 36] obtained in recent years, provides a quantitative description of the nonmonotone temperature dependence of the solubility of C_{60} in different solvents, as observed in Ref. [7]. A decrease in solubility with temperature is observed in the temperature range where the existence in the solution of clusters consisting of a large number of fullerene molecules is thermodynamically beneficial. This decrease may be treated as a result of thermal decomposition of the largest clusters with rising temperature. A further increase in temperature should have brought about a rise in solubility; however, as follows from the calculation results, the minimum of solubility for the above-determined values of the parameters A and B is reached at $T \approx 4000$ K, when neither the solvent nor fullerenes exist any longer. In the low-temperature range ($T < 260$ K) the clusters are of little importance, which is caused by a different crystalline structure of the fullerene in the solid phase and the relatively higher value of the energy of interaction between fullerene molecules and their surroundings.

It is of interest to pay attention to the considerable distinction between the temperature dependences of the solubility of fullerenes C_{60} and C_{70}. As distinct from the case of C_{60} considered above, the solubility of C_{70} monotonically increases with rising temperature everywhere over the temperature region where the measurements were performed. This can be treated as a consequence of the higher magnitude of the difference in energy of interaction of the fullerene C_{70} with its surroundings in a solution and in a solid in comparison with that of C_{60}. Indeed, on the one hand, the difference in the energy of interaction of molecules C_{60} and C_{70} with adjacent solvent molecules is roughly proportional to the difference in the surface areas of those molecules. On the other hand, these molecules form approximately similar crystal structures in corresponding fullerites. So, the difference in the interaction energy of a fullerene molecule with its surroundings in a solution and in a crystal in the case of C_{70} should exceed that in the case of C_{60}. In such a situation the formation of clusters consisting of a number of fullerene molecules in the solution of C_{70} is hardly possible, which is confirmed by the rising temperature dependence of the solubility of C_{70}. The higher the solubility of fullerene in the specific solvent, the greater the energy difference. Therefore it can be assumed that for solvents dissolving C_{70} more weakly than toluene, xylene and CS_2, shown in Fig. 2, the role of aggregates should rise. Experimental data revealing this assumption will be given below.

2.4 Heat of solution of fullerene C_{60}

The noted above tendency of fullerenes in solution to form clusters is reflected in the magnitudes of parameters governing their properties in the conditions under consideration. Thus, the existence of the dependences of the cluster size distribution function on the concentration and temperature of the solution leads to corresponding concentration and temperature dependences of thermodynamic and kinetic parameters characterizing the behavior of fullerenes in solutions. Specifically, in this section of the article it is shown that this phenomenon causes the concentration and temperature dependences of the heat of solution of fullerenes.

Using the approach developed above, let us state the form of the cluster size distribution function in an unsaturated solution. In this case a solid phase is absent, so that the distribution function is determined through the equilibrium condition for clusters of various sorts in a solution. Using equation (3) derived above for the chemical potential of a cluster in a solution, we can obtain the expression for the cluster size distribution function in the unsaturated solution of fullerenes, depending on the solution concentration [37]:

$$f_n(C) = \lambda^n \exp\left(\frac{-An + Bn^{2/3}}{T}\right). \tag{8}$$

Here the parameters A and B were determined above and the parameter λ depending on the concentration of a solution is determined through the normalization condition

$$C = C_0 \int_{n=1}^{\infty} n\lambda^n \exp\left(\frac{-An + Bn^{2/3}}{T}\right) \mathrm{d}n\,. \tag{9}$$

The coefficient C_0 defines the absolute magnitude of the solution concentration and can be found by requiring (in specific conditions) the concentration determined through expression (9) to be its saturated value which is expressed through (5). The cluster size distribution functions in solution of fullerene C_{60}, calculated on the basis of equations (6), (8) at various concentrations and temperatures, are shown in Figs 3, 4. As is seen from the data presented, the average size of a

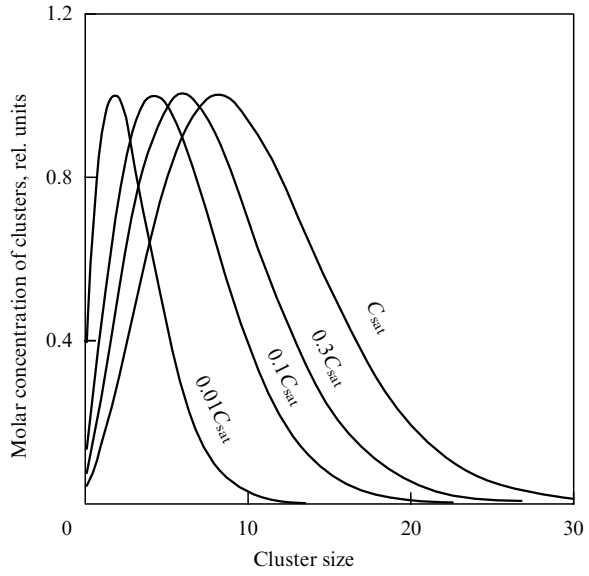

Рис. 4. Concentration dependence of the cluster size distribution function in a solution of C_{60} fullerene, calculated from the cluster droplet model for $T = 350$ K.

cluster in a fullerene solution decreases gradually as the solution concentration is lowered. The lowering of the concentration by two orders of magnitude relating to the saturation value still does not violate the condition of validity of the droplet model ($n \gg 1$) for description of the behavior of clusters in solution. At concentrations three orders of magnitude lower than the saturation value, clusters practically do not form and only isolated fullerene molecules exist in the solution.

The form of the temperature dependence of solubility of fullerenes in solvents under consideration shows the existence of both temperature and concentration dependences of the heat of solution of fullerenes in these solvents. This also follows from the concentration and temperature dependences of the cluster size distribution function in solutions, which are shown in Figs 3, 4. The concentration dependence of the heat of solution may provide an explanation for the observed contradiction between experimental data concerning the heat of solution of fullerenes [38–40].

In terms of the above-described droplet model of a cluster in a fullerene solution, the energy of formation of a cluster consisting of n fullerene molecules is determined by the following expression

$$E_n = n(An - Bn^{2/3}), \tag{10}$$

where the constants A and B were determined above. Using the expression for the cluster size distribution function, we obtain the formula governing the thermal effect of solution of fullerenes per mole of dissolved substance:

$$H = \frac{\sum_{n=1}^{\infty} E_n f_n(C)}{\sum_{n=1}^{\infty} n f_n(C)} N_a = \frac{\sum_{n=1}^{\infty} n(An - Bn^{2/3})\lambda^n \exp\left[(-An + Bn^{2/3})/T\right]}{\sum_{n=1}^{\infty} n\lambda^n \exp\left[(-An + Bn^{2/3})/T\right]} N_a, \tag{11}$$

where the constant parameter λ is determined by the total concentration of the solution formed through the normalization condition (9). The concentration and temperature dependences of the heat of solution calculated on the basis of equation (11) for the fullerene C_{60} in toluene, benzene and CS_2 are given in Fig. 5.

The data presented permit the conclusion that the cluster formation considerably affects the heat of solution of fullerenes. Thus, for a solution containing only isolated fullerene molecules (concentration of solution less than 0.1% of saturated), the heat of solution comprises -5.6 kJ mol^{-1}, whereas for that with concentration 15% (average size of clusters in the solution is equal to 7) the heat of solution comprises -10.6 kJ mol^{-1}. Apparently, the discrepancy between various experimental data on the heat of solution of fullerenes [38–40] may be ascribed to such a sharp concentration dependence of the heat of solution of fullerenes.

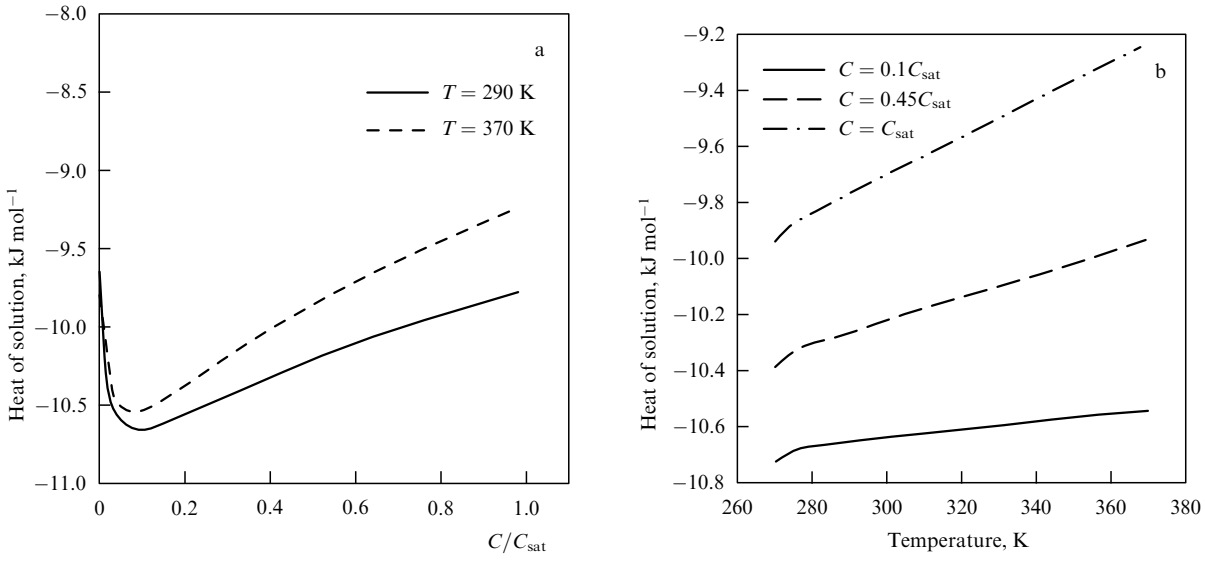

Рис. 5. Concentration (a) and temperature (b) dependences of the heat of solution of fullerenes in toluene, benzene, and CS_2, calculated using the droplet model and expression (11).

As follows from the given data, cluster formation in fullerene solutions has a considerable impact on the thermal effect in a solution and results in concentration and temperature dependences of the heat of solution. This phenomenon should be taken into consideration in measuring the thermal effect of solution of both fullerenes and other substances forming aggregates in solutions. On the other hand, the existence of a concentration dependence of the heat of solution of a substance may be used as evidence of the cluster origin of solubility of this substance.

3. Transfer phenomena in fullerene solutions

3.1 Diffusion of fullerenes in solutions

Diffusion coefficient. The diffusion coefficient is an important parameter characterizing the behavior of fullerenes in a solution. This parameter governs the optimum conditions of crystallization of fullerenes in solutions, as well as the possibility of their separation and purification. The results of measuring the diffusion coefficients of C_{60} and C_{70} in some solvents are given in Table 4. It is interesting to compare these data with a simple estimate that may be obtained on the basis of Stokes' formula describing the diffusion of a spherical particle in a viscous fluid:

$$D = \frac{kT}{6\pi\eta r_s} . \tag{12}$$

Here, T is the temperature of the liquid, η is its dynamic viscosity, and r_s is the particle radius. The condition of validity of this equation can be reduced to the requirement of low magnitudes of the Reynolds number for a diffusing particle:

$$\mathrm{Re} = \frac{\bar{r}_s \bar{v} \rho}{\eta} \ll 1 , \tag{13}$$

where $\bar{v} \approx T/m$ is the characteristic velocity of a particle, m is its mass, and ρ is the mass density of the solvent. Using the obvious interconnection between the mass of a particle and its radius, this expression can be presented as a limiting condition for the minimum radius of a diffusing particle

$$r_s \gg \frac{T\rho^2}{\eta^2 \rho_p} , \tag{13a}$$

where ρ_p is the mass density of the particle. Using the characteristic magnitudes of the viscosity of typical organic solvents $\eta \sim (1-3)\times 10^{-3}$ N s m^{-2}, we obtain that the limitation shown above is reduced to the requirement $r_s \gg 10^{-10}$ cm, which is valid for all practical purposes.

The values of the radius r_s, determined on the basis of formula (12) from the experimental data for the diffusion coefficient of fullerenes in various solvents, are given in the penultimate column of Table 4. One can see that these values substantially exceed the true radius of a C_{60} molecule, which is equal to 0.35 nm. In addition, the differences in the radius values obtained for different solvents seem to be striking. These differences may be attributed to the effect of aggregation of fullerenes in solutions, discussed in detail above. Apparently, this effect has a universal origin, although the data listed in Table 4 are indicative of considerable differences between the characteristic sizes of fullerene clusters in different solvents.

Concentration dependence of the diffusion coefficient of fullerenes in solutions. The existence of fullerenes in solutions in the form of clusters, whose average size depends on the concentration of the solution, suggests the dependence of the diffusion coefficient of fullerenes in a solution on their concentration [37]. Indeed, in the case of a solution of low concentration almost no clusters are formed and the diffusion coefficient is close to the corresponding value for a single fullerene molecule. As the concentration of fullerenes in the solution rises, the average cluster size increases and, consequently, the diffusion coefficient of fullerenes decreases in accordance with expression (12).

Let us calculate the concentration dependence of the diffusion coefficient of fullerene C_{60} in solutions having regard to cluster formation. We will use here the results of the approach developed above to the establishment of the cluster size distribution function [11, 12, 16, 37]. According to this approach, the cluster size distribution function for the saturated solution is expressed through equation (4), whereas

Table 4. Diffusion coefficient of fullerenes in solutions.

Solvent	Diffusion coefficient, 10^{-6} cm^2 s^{-1}	T, K	r_s, A	Ref.
		Fullerene C_{60}		
chlorobenzene	3.7 ± 0.7	295	7.4	[41]
1, 2-dichlorobenzene	1.1 ± 0.2	295	7.7	[41]
pyridine	3.1 ± 0.6	295	7.1	[41]
pyridine/acetonitrile (9/1)	3.4 ± 0.7	295	7.5	[41]
pyridine/acetonitrile (8/2)	3.8 ± 0.7	295	7.4	[41]
pyridine/acetonitrile (6/4)	4.1 ± 0.8	295	8.3	[41]
pyridine/acetonitrile (4/6)	5.1 ± 1.0	295	8.2	[41]
benzonitrile	1.4 ± 0.3	295	12.4	[41]
dichloromethane	4.4 ± 0.9	295	11.1	[41]
tetrahydrofuran	1.6 ± 0.3	295	25.0	[41]
benzene	9.1	298		[42]
CS_2	18.5	298		[42]
		Fullerene C_{70}		
CS_2	16.6	298		[42]
benzene	8.3 ± 7	298		[43]

for an unsaturated solution it is expressed through formula (8). Let us determine the diffusion coefficient D of fullerenes in a solution using the standard approach based on the formula

$$J = -D\nabla C\,. \tag{14}$$

Here J is the flux of matter in the solution under the action of concentration gradient. In view of the cluster origin of solubility of fullerenes, we represent expression (14) in the form of the sum

$$J = \sum_n J_n = -\sum_n D_n \nabla C_n n\,, \tag{15}$$

where J_n, D_n and C_n are the partial values of the flux, diffusion coefficient and concentration of the cluster of size n, respectively.

We will derive the relationship between the diffusion coefficient D_n of the cluster of size n and its radius r_n based on the droplet model of a cluster, the Stokes' formula (12) and the obvious relation

$$r_n = \left(\frac{3Mn}{4\pi\rho}\right)^{1/3}, \tag{16}$$

where M is the mass of the fullerene molecule, and ρ is the cluster density. By combining relations (14)–(16) and using the cluster size distribution function (8), we derive the expression for the diffusion coefficient of the fullerene in view of the possibility of cluster formation:

$$D = D_0 \frac{\int_{n=1}^{\infty} n^{5/3}\lambda^{n-1}\exp\left[(-An + Bn^{2/3})/T\right]\mathrm{d}n}{\int_{n=1}^{\infty} n^{2}\lambda^{n-1}\exp\left[(-An + Bn^{2/3})/T\right]\mathrm{d}n}\,. \tag{17}$$

Here D_0 is the diffusion coefficient of an isolated fullerene molecule. The concentration dependence of the cluster size distribution function points to a pronounced concentration dependence of the diffusion coefficient of fullerenes in a solution. The results of calculation of this dependence, performed using expression (17), are given in Fig. 6. As is seen, the cluster formation in a solution close to saturation leads to a decrease in the diffusion coefficient by approximately 30% as compared with the corresponding value of D_0 for an isolated molecule.

Diffusion separation of fullerenes in a solution. The concentration dependence of the diffusion coefficient of fullerenes in solutions notably complicates their kinetic behavior. Specifically, if a solution contains a mixture of different sorts of fullerene molecules, the character of diffusion of molecules of a given sort is essentially determined by their propensity to the cluster formation in a solution. In the most typical, for practical purposes, situation a solution contains a fullerene of a specific sort with a small admixture of fullerene molecules of another sort (for example, C_{60} with a small admixture of C_{70} or higher fullerenes). In this case the molecules comprising a small admixture to the basic substance do not practically form clusters and are characterized by the diffusion coefficient, which is inherent to isolated molecules. The molecules of basic substance, whose concentration is close to saturated, have a tendency to the aggregation. In accordance with the results obtained above, the diffusion coefficient for this substance considerably exceeds that for an isolated molecule and exhibits by the decreasing temperature dependence.

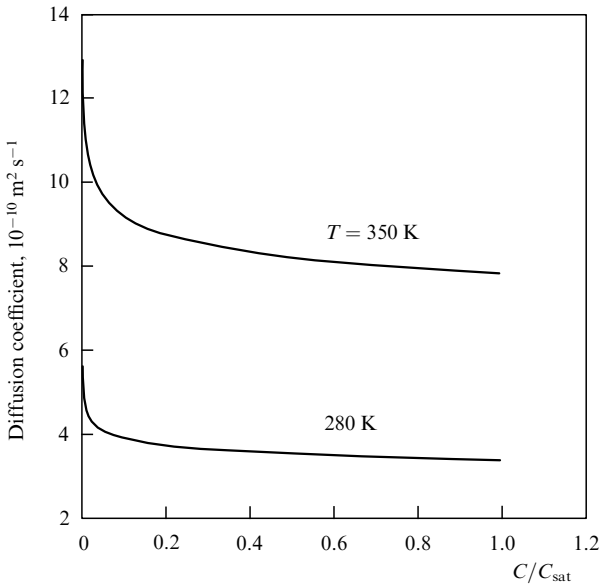

Рис. 6. Concentration dependence of the diffusion coefficient of fullerene C_{60} in toluene.

The difference in the diffusion coefficients of fullerene molecules of different sorts makes us think of a possibility for developing the diffusion methods of enrichment, separation and purification of fullerenes. We will now analyze the possibility of using the above-determined concentration dependence of the diffusion coefficient of fullerenes in a solution as a basis for the diffusion method of enrichment of fullerenes in a solution containing fullerenes of two types with highly differing concentrations. In this case, the fullerene which is present in the solution as a minor impurity and, therefore, does not form clusters must have a higher diffusion coefficient than the fullerene whose concentration is close to saturated and which is present in the solution in the form of large clusters.

Let us analyze the one-dimensional nonstationary problem on the diffusion of fullerenes in a solution with allowance made for the concentration dependence of the diffusion coefficient as determined above [44]. We shall assume that the source of fullerenes is provided by a plane layer of a solid material constituting the mixture of fullerenes of two sorts, in which fullerene molecules of a certain sort predominate, whereas the molecules of the other sort make up only a minor impurity. In this case, as follows from the results of the foregoing calculation, one can assume that the molecules of minor impurity form almost no clusters and are characterized by the diffusion coefficient D_0 inherent to an isolated molecule. The diffusion coefficient of fullerene molecules of the predominating sort depends on the concentration and due to the possibility of forming clusters in the solution is less than the diffusion coefficient of isolated molecules. The diffusion equations for fullerenes of the predominating sort (concentration C_1) and of the minor impurity (C_2) have the standard form

$$\frac{\mathrm{d}}{\mathrm{d}x} D_1(C_1)\frac{\mathrm{d}C_1}{\mathrm{d}x} + \frac{\mathrm{d}C_1}{\mathrm{d}t} = 0\,, \tag{18}$$

$$D_2\frac{\partial^2 C_2}{\partial x^2} + \frac{\partial C_2}{\partial t} = 0\,. \tag{19}$$

Here D_1 and D_2 denote the diffusion coefficients for the first and second components, respectively. Equations (18) and (19) have automodelling solutions dependent on the single variable $x/\sqrt{t}$; however, in the case of the concentration dependence of the diffusion coefficient, this solution calls for numerical calculations. Equation (18) was solved with the initial conditions

$$C_1(x=0,\ t=0)=C_1^*\,,\quad C_1(t=0)=0\,,\quad C_1(x=\infty)=0\,, \tag{20}$$

which correspond to one-dimensional diffusion from an instantaneously 'actuated' plane source. Here C_1^* is the saturated concentration of fullerenes in the solution. The solution of equation (19) with the initial conditions

$$C_2(x=0,\ t=0)=C_1^0\,,\quad C_2(t=0)=0\,,\quad C_2(x=\infty)=0 \tag{21}$$

is known quite well at $C_2^0 \ll C_1^*$:

$$C_2=\frac{K}{(4\pi Dt)^{1/2}}\exp\left(-\frac{x^2}{4Dt}\right), \tag{22}$$

where K is the normalization factor.

In Figure 7, the solutions to equations (18) and (19) are given in the form of spatial dependences of the fullerene enrichment factor η defined in the standard manner as

$$\eta=\frac{C_2(x,t)C_1(x=0,\ t=0)}{C_1(x,t)C_2(x=0,\ t=0)}\,. \tag{23}$$

We have neglected the insignificant difference between the diffusion coefficients of isolated fullerene molecules of different sorts, which is due to some variations in their sizes. This difference amounts to several percent, which is within the accuracy of the cluster droplet model employed.

As follows from the calculated results, the enrichment factor of fullerenes in a solution some time-dependent distance x^* away from the source assumes the maximum value η_m. In this case due to the automodelling character of the solutions of equations (18) and (19), the quantity η_m is time-independent and close to 20.

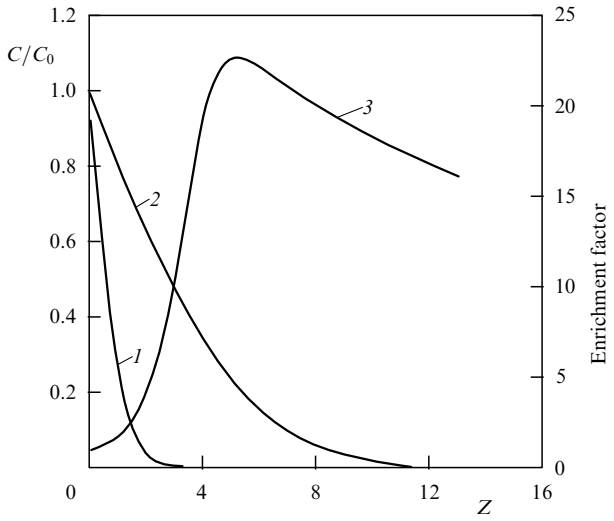

Рис. 7. Dependences of the relative concentrations of fullerene C_{60} (*1*) and a small addition of a higher fullerene (*2*) diffused in a toluene solvent, and also of the enrichment factor (*3*) on the automodelling variable $z=x/(D_0t)^{1/2}$ for $T=303$ K.

The results obtained permit us to imagine the possible schemes of diffusion enrichment of fullerenes in a solution. In so doing it appears appropriate to use the great experience accumulated in the development of the technology of isotope separation [45, 46]. We shall first consider the scheme based on nonstationary diffusion. A container filled with a solvent is divided into two parts with a porous partition that does not retard the diffusion motion of dissolved molecules but prevents convective stirring of the solution in two parts of the container. A solid mixture of a fullerene (for example, C_{60}) with a minor impurity of a higher fullerene is placed at the bottom of one of the container parts. Due to the difference in the diffusion coefficients of fullerenes of different sorts, the fullerene mixture penetrating into the second part of the container has to be highly enriched with the minor impurity. After a lapse of time corresponding to the maximum value of the enrichment factor for the given system geometry, the second part of the container, filled with the enriched solution, rapidly drains. Thereby, the fullerene extract is enriched with the minor impurity in a single-action mode.

In practice it may be proved that the scheme of diffusion enrichment of fullerenes in the stationary mode is more convenient. In this case, an elementary separation cell likewise consists of two volumes divided by a porous partition. An initial solution containing fullerene molecules of two sorts is slowly pumped through one part of the cell. A pure solvent is pumped in the opposite direction through the other part of the cell. As a result of diffusion through the porous partition, the solution in the second part of the cell is enriched with the minor impurity. In so doing, the maximum enrichment factor corresponds to the ratio between the diffusion coefficients for the two components of the solution. Because this ratio is approximately equal to 1.3, a multistage system must be used to attain a more significant enrichment factor. In such a scheme, the relationship between the resultant enrichment factor η_f and the number m of stages is given by the known relation

$$\eta_f=\eta_0^m\,,$$

where η_0 is the enrichment factor for a single cell.

It should be noted that in using here diffusion methods for fullerene enrichment the final degree of enrichment depends on whether the fullerene molecules comprising a minor admixture tend to aggregate. If such a tendency is absent, as is apparently the case for fullerene C_{70} in such solvents as toluene, benzene, CS_2, etc., quite a high degree of enrichment can be reached.

In a more general case, where the fullerene molecules of both sorts have a tendency to aggregation, the enrichment degree relating to the minor admixture as a rule can hardly exceed 50%. Indeed, as the concentrations of components of the mixture approach one another, the average sizes of the clusters and, consequently, the diffusion coefficients for molecules of the two sorts are approached as well. This makes the considered method for fullerene enrichment inapplicable. However, in any event the method considered can be applied validly to removal of minor impurity from the mixture of fullerenes of different sorts.

Therefore, the tendency of fullerenes to cluster formation in a solution is reflected in the diffusion behavior of fullerenes in a solution and is responsible for the concentration

dependence of the diffusion coefficient. This dependence is calculated through the droplet cluster model, which has showed itself to advantage previously in interpreting the nonmonotone temperature dependence of solubility of fullerenes. The derived concentration dependence of the diffusion coefficient of fullerenes in a solution may be used as a basis for diffusion fullerene enrichment or for purification of fullerenes. This method appears most convenient in enrichment of a solution containing the mixture of C_{60} with a minor impurity of higher fullerenes.

3.2 Thermal diffusion of fullerenes in solutions

As revealed by the model calculations described above, fullerenes in solutions have a tendency to form aggregates or clusters, whose average size depends on the concentration and temperature of the solution. The temperature and concentration dependences of the cluster size distribution function show the possibility of exhibition of a new mechanism of thermal diffusion of fullerenes in solutions. A simple approach to the evaluation of the thermal diffusion coefficient proceeding from the above-determined temperature and concentration dependences of the cluster size distribution function is presented below [47, 48].

We shall define the thermal diffusion coefficient D_T of fullerenes in a solution in a standard manner, expressing the relation between the thermal diffusion flux J_T and the temperature gradient in the solution as

$$J_T = -C\frac{D_T}{T}\nabla T. \tag{24}$$

We shall assume that the time required for equilibration of cluster size distribution function defined by relations (4) and (8) is much less than the time required for smoothing spatial temperature nonuniformities. Thereby, we assume the existence of local thermodynamic equilibrium in the solution. By virtue of relations (4) and (8), the temperature gradient in the solution causes gradients in partial concentrations of clusters. This, in turn, causes diffusion flows proportional to the temperature gradient. In accordance with the foregoing, the partial diffusion flux of clusters of size n, due to the presence of the temperature gradient, is expressed by the relation

$$J_n = -D_n\nabla C_n = -\frac{\nabla T}{T}D_n\left(\frac{-An + Bn^{2/3}}{T}\right)f(n), \tag{25}$$

where the cluster size distribution function $f(n)$ is given by relation (4) or (8), depending on whether the solution is saturated or not. Using this notation, it is assumed as is usually accepted in the statistical physics that the main temperature dependence of the cluster size distribution function is in the exponential factor. The net diffusion flux is calculated through the summation (integration) of the expression (25) over n, which permits using equation (24) to determine the thermal diffusion coefficient.

The diffusion coefficient D_n of clusters of size n in the solution will be determined again using the Stokes' formula (12) which adequately describes the experimental data. Then, the expression for the thermal diffusion coefficient of fullerenes in the solution assumes the form

$$D_T = D_0\int_1^\infty \frac{-An + Bn^{2/3}}{T}\frac{f(n)}{n^{1/3}}\,dn, \tag{26}$$

where the distribution function $f(n)$ is given by formulae (4), (8) and has to be calculated by numerical methods. The results of calculations, performed for different values of temperature and concentration of the solution of fullerene C_{60} in toluene on the basis of the previously determined cluster size distribution functions (4) and (8) using relations (12), (25), and (26), are given in Fig. 8. One can see that the effect of thermal diffusion shows up in the temperature range above 260 K. This is a consequence of aggregation of fullerenes in the solution, which as shown above plays a significant role in the above-identified temperature range.

It should be noted that only one of the possible mechanisms of thermal diffusion of fullerenes in a solution was treated. This mechanism relating to the aggregation phenomenon in fullerene solution is inherent specifically to fullerenes and has no general origin. Another mechanism, not treated here, is of a more general nature and shows up even in the case of isolated fullerene molecules. This mechanism is caused by the larger size of a fullerene molecule as compared with the solvent molecule. We shall now evaluate the thermal diffusion coefficient for this latter mechanism. In the presence of a temperature gradient, a fullerene molecule is subjected to the action of a force which is proportional to the corresponding difference of pressures acting from the side of fluid on two opposing hemispheres of the molecule. This causes a directed drift of molecules, whose velocity w may be estimated through the Stokes' formula

$$w = \frac{\nabla T}{4\pi\eta r}, \tag{27}$$

where r is the radius of the fullerene molecule. This results in the estimation of the thermal diffusion coefficient according to the mechanism in question:

$$D_T \approx \frac{T}{4\pi\eta r}. \tag{28}$$

Expression (26) differs from this estimate by a factor $(-An + Bn^{2/3})/T$, which is much greater than unity. One

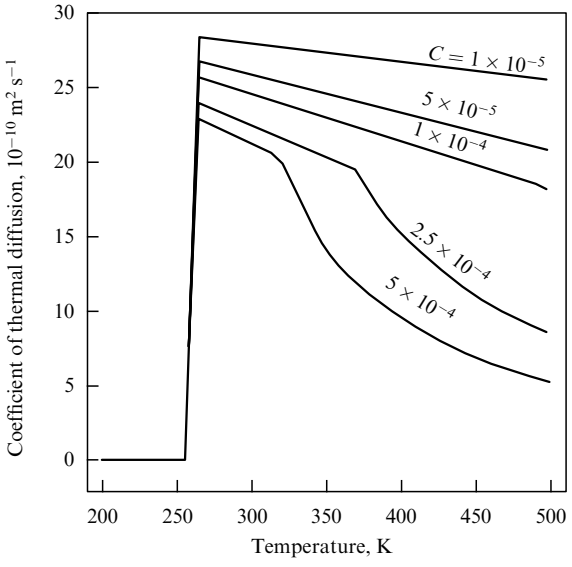

Рис. 8. Dependences on temperature of the coefficient of thermal diffusion of fullerene C_{60} in a toluene solvent, calculated for various solution concentrations and allowing for the appearence of fullerene clusters.

can see that under conditions favorable to cluster formation the mechanism of thermal diffusion, associated with the effect of aggregation of fullerenes in a solution, proves much more efficient as compared with the more general mechanism which does not relate to this effect.

4. Optical properties of fullerenes in solutions

4.1 Nonlinear optical susceptibility

The aggregation phenomenon considered above essentially affects the optical properties of fullerenes. This is caused by differences in the optical characteristics of isolated fullerene molecules and of those involved in aggregates in solutions. Further, it appears to be obvious that the optical properties of aggregates depend on their sizes. Therefore the optical properties of a fullerene solution are determined by the cluster size distribution function, and all the factors modifying this function have a considerable influence on the optical properties of fullerenes.

The simplest manifestation of effects of such a kind was described in detail in one of the earliest publications [8] related to the experimental exploration of optical properties of fullerenes in solutions. In this work, the concentration dependence of the third-order nonlinear optical susceptibility for C_{60} dissolved in benzene was measured. The nonlinear response was measured versus the concentration of solution using an Nd-glass laser ($\lambda = 1.064$ μm) with a pulse energy of 5 mJ and duration of 50 ps. The measured results are given in Fig. 9. As is seen, the measured value of the susceptibility (per C_{60} molecule) $\chi^{(3)} \approx 10^{-38}$ $m^2\,V^{-2}$ exceeds by about 3 orders of magnitude the estimated value of this parameter for the case of nonresonant response of optical electrons $\chi^{(3)}_{nr} \sim \chi^{(1)} E_a^{-2} \sim 10^{-41}\,m^2\,V^{-2}$, where $E_a \sim e/a_0 \sim 5 \times 10^{11}\,V\,m^{-1}$ is the characteristic atomic electric field strength. This shows the resonant nature of interaction of the laser radiation with electrons belonging to a fullerene molecule.

Another peculiarity of the experimental data presented in Fig. 9 concerns the nonlinear behavior of the concentration dependence $\chi^{(3)}(C)$. The observed deviation of the dependence from a straight line shows the decrease in the portion of fullerene molecules interacting with the laser radiation in a resonant manner as the solution concentration increases. Such a peculiarity is related to the aggregation of fullerenes in solution, as a result of which the resonant four-photon mixing frequency is shifted [49]. Fullerene molecules involved in clusters are excluded from the process of resonant interaction with laser radiation, which in turn results in the saturation of the concentration dependence of the nonlinear response.

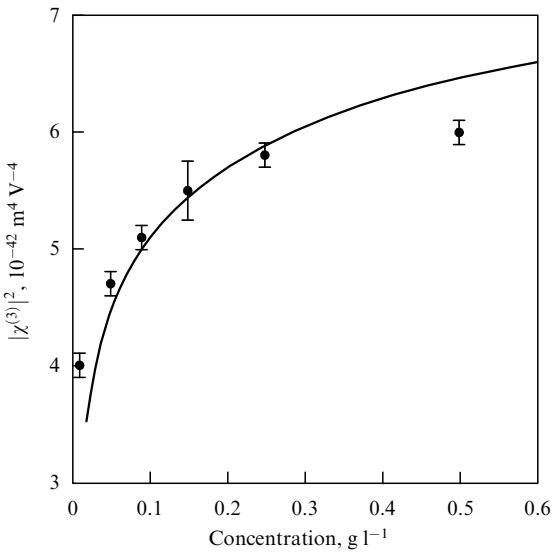

Рис. 9. Concentration dependence of the third-order nonlinear optical susceptibility of fullerene C_{60} in a benzene solution. The solid line shows the results of calculation.

The above-described mechanism of the influence of the fullerene aggregation on the shape of the concentration dependence of the third-order nonlinear optical susceptibility is confirmed by the calculated results [49] produced using the above-stated concentration dependence of the cluster size distribution function (see Section 3). These results having the form of the concentration dependence (in relative units) of the portion of isolated fullerene molecules (not incorporated into clusters) are shown in Fig. 9 by the solid line. As is seen, this dependence closely agrees with the results of measuring of the concentration dependence of the third-order nonlinear optical susceptibility [8]. Such an agreement permits the statement that the fullerene molecules involved in clusters are removed from the region of resonant interaction with laser radiation, accompanied by the four-wave mixing effect.

The above-stated effect of displacement of the resonant frequency of the four-wave interaction as a consequence of the aggregation of fullerenes in solution permits the use of measured concentration dependences of the third-order nonlinear optical susceptibility for resolution of the issue on the possible aggregation of fullerene molecules of a specific sort in a particular solution. Specifically, it would be interesting to try to state a connection between the solvatochromic phenomena, observed in solutions of fullerenes C_{60} and C_{70} in various solvents in the works [9, 10], and the behavior of the parameter $\chi^{(3)}$ depending on the concentration of solution. Further, it appears to be attractive to perform the measurements of this parameter in the conditions of experiments [13, 14], where the slow, over tens of days, formation of fractal aggregates of C_{60} in benzene solution was observed. The magnitude of the displacement of the four-wave mixing resonant frequency for large fractal aggregates may be found not so significant as in the above-analyzed case of small-sized compact clusters, which is reflected on the form of time dependence of $\chi^{(3)}$.

4.2 Solvatochromism

The experimentally discovered phenomenon of solvatochromism can be considered as one of the most interesting from the scientific viewpoint properties of fullerenes in solutions. This phenomenon manifests itself in a sharp change of the optical or Raman spectrum of a solution of fullerenes C_{60} or C_{70} as a result of a slight variation in the solution concentration or solvent content [9, 10]. These peculiarities in the behavior of fullerenes in solutions are observed in the case of using a binary mixture as a solvent. In this case the tendency of fullerenes to aggregation shows itself as the significant dependence of the cluster size distribution function not only on the solution concentration but also on the content of the solvent. This, in turn, causes a dependence of the absorption optical spectra of fullerenes in solutions on the solvent content. In certain conditions this dependence has a critical character, which is exhibited in a sharp qualitative

change of the spectral features under a slight variation of the solution concentration or solvent content.

This peculiarity in the behavior of fullerenes in solutions was first observed in measuring the electronic absorption spectra of fullerene C_{70} dissolved in the mixture of acetonitrile and toluene [9]. The measured results, given in Fig. 10, show the critical character of the dependence of the spectrum on the solvent content. Thus, as the volume content of acetonitrile in the solvent exceeds 60%, the electronic absorption spectrum of C_{70} shows additional features which are not observed at a lower concentration of acetonitrile. A strong absorption band in the wavelength range 550–800 nm appeared, whereas the fine structure in the wavelength range 300–400 nm of the absorption spectrum essentially disappeared. The indicated peculiarities in the behavior of C_{70} spectra in binary solutions were attributed by the authors [9] to the possibility of forming clusters consisting of a number of fullerene molecules in the solutions.

A detailed exploration of the solvatochromism phenomenon in solutions of fullerene C_{70} was performed in the subsequent work [50], where in parallel with the absorption and fluorescence spectra of solutions of fullerenes C_{60} and C_{70} in a mixture of solvents of various content the cluster size distribution function was also measured. In Figure 10, the results of measuring electronic absorption spectra of C_{70} dissolved in the mixtures of acetonitrile with toluene under various conditions are given. The similar peculiarities were observed for fullerene C_{60} dissolved in the mixtures of acetonitrile with toluene at various solution content. As is turned out, the absorption spectra of dissolved fullerenes C_{60} and C_{70} undergo considerable alterations as a result of change in both the solvent content and solute concentration. Specifically, the excess in concentration of acetonitrile mixed with toluene above 70% results in a considerable red shift and broadening of the maximum in the absorption spectrum of fullerene. The rise in the concentration of acetonitrile in the mixture of benzonitrile and acetonitrile causes the smoothing of the feature in the absorption spectrum of C_{70} at $\lambda = 480$ nm and the appearance of a broad band with maximum near 590 nm. Addition of 70% acetonitrile into toluene causes the red shift of the absorption spectrum of C_{60}, so that the feature observed at $\lambda = 404$ nm becomes less pronounced, whereas that at $\lambda = 600$ nm disappears at all. Using the mixtures of benzene with hexane and benzonitrile with hexane as solvents no alterations in the absorption spectra of C_{70} were observed.

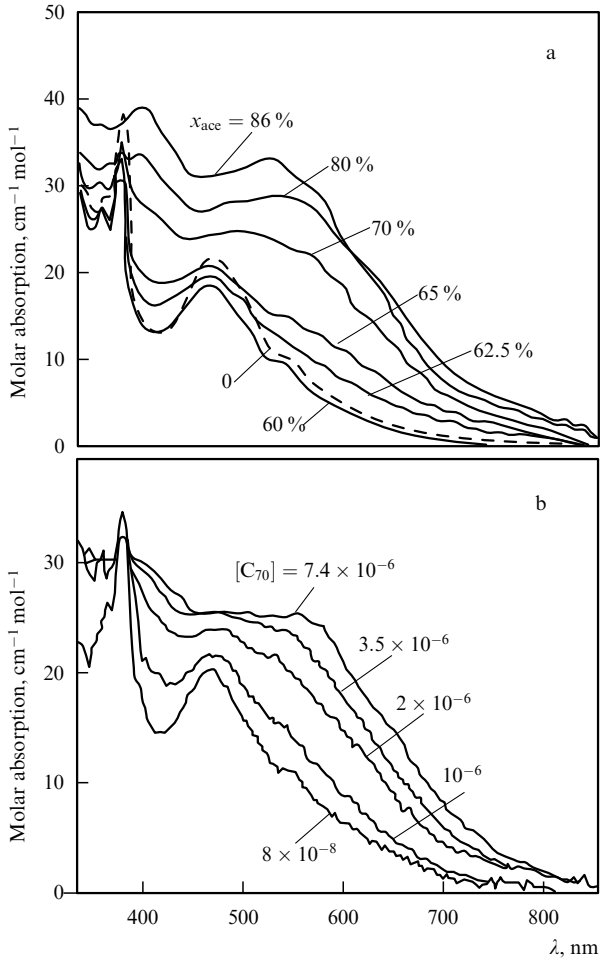

Рис. 10. Absorption spectra of C_{70} dissolved in a mixture of acetonitrile and toluene, measured at various concentrations of acetonitrile in the mixture x_{ace} (a) (molar concentration of fullerene $M = 6.6 \times 10^{-6}$) and different concentrations of solution [C_{70}] (b) for $x_{ace} = 70$ %.

As is shown in measurements performed in the above-cited work [50], the change in the solvent content causes considerable alterations in not only absorption spectra, but also fluorescent spectra of fullerenes. This can be seen from the comparison of excitation and emission spectra of fullerene C_{70} dissolved in pure toluene and in mixtures of toluene with acetonitrile of various content, presented in Fig. 11. As acetonitrile is added to the solution the fluorescence intensity of C_{70} at $\lambda = 664$ nm notably lowers, whereas the intensity of light scattering with a maximum at wavelength 552 nm rises about 100 times. Further, in the fluorescent spectrum two additional peaks appear at $\lambda = 595$ and 638 nm. Similar measurements performed using mixtures of benzonitrile with acetonitrile, benzene with methanol, and dichlorobenzene with acetonitrile as solvents also show a decrease in the fluorescence intensity and an increase in the scattering intensity as a result of a rise in the concentration of the component which does not dissolve the fullerenes. Using mixtures of benzene with hexane and benzonitrile with hexane as solvents, both components of which dissolve fullerenes quite well, no dependence of the luminescence spectra of C_{70} on the content of a solvent was found.

The reason behind the above-described solvatochromism phenomena, inherent to the behavior of fullerenes in multi-component solutions, lies in the tendency of fullerenes to cluster formation. This follows from the results of direct measurements of the cluster size distribution function performed for C_{70} dissolved in the mixture of toluene with acetonitrile of various content and concentration, using the dynamic light scattering method [50]. These results are given in Fig. 12. As can be seen, the average size of clusters increases both as the content of acetonitrile rises and the solution concentration is enhanced. Further, a bimodal form of the cluster distribution in solution of specific concentration and acetonitrile content engages our attention. Two kinds of clusters are observed: large, 100 nm in diameter (under different conditions — 1000 nm) and small, 3 nm in diameter (under different conditions — 100 nm). Apparently, small clusters serve as a building material for larger structures. The absence of clusters of intermediate size shows the instability of such formations, the reason for which is still to be found.

Therefore, it can be stated that the solvatochromism phenomena observed in fullerene solutions originate from

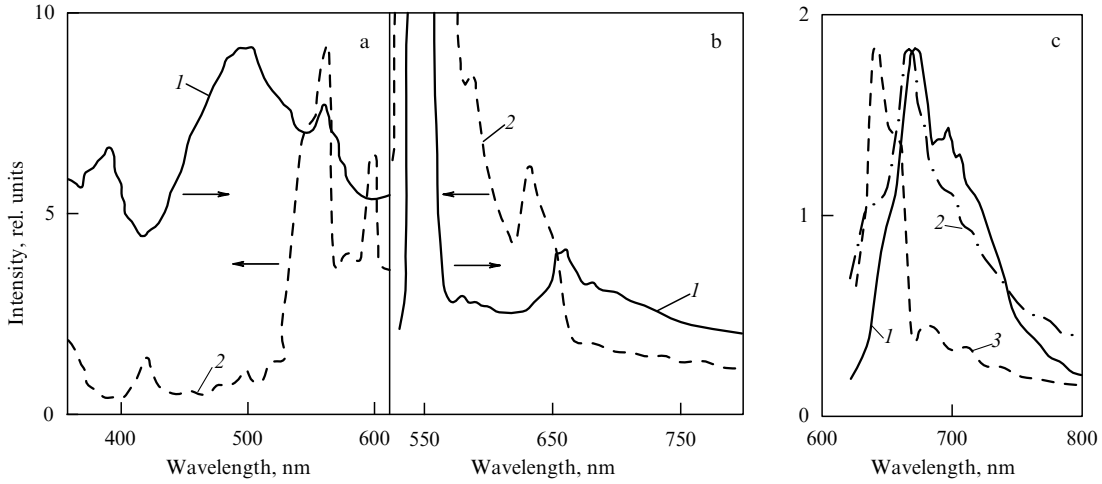

Рис. 11. Excitation spectrum of the C_{70} fullerene in a mixture of toluene and acetonitrile: *1* — 100 % toluene ($\lambda_{em} = 664$ nm); *2* — 30 % toluene ($\lambda_{em} = 638$ nm) (a). Emission spectrum of C_{70} ($\lambda_{ex} = 550$ nm): *1* — no acetonitrile; *2* — 70 % acetonitrile (b). Emission spectrum of C_{70} ($\lambda_{ex} = 550$ nm): *1* — no acetonitrile; *2* — 50 % acetonitrile; *3* — 90 % acetonitrile; $[C_{70}] = 3.5 \times 10^{-6}$ mol l^{-1} (c).

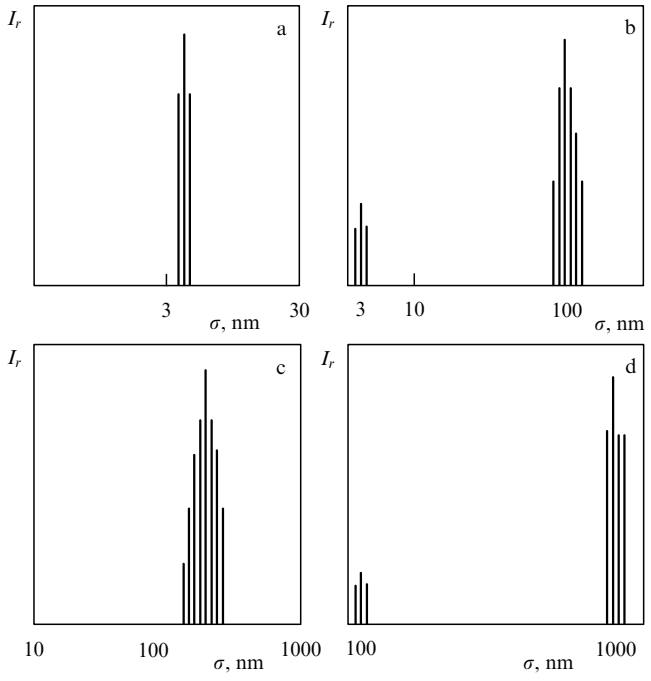

Рис. 12. Size distribution of C_{70} fullerene clusters in the following acetonitrile and toluene mixtures: (a) 100 % toluene; (b) 70 % acetonitrile, $[C_{70}] = 3.5 \times 10^{-6}$ mol l^{-1}; (c) 70 % acetonitrile, $[C_{70}] = 6 \times 10^{-6}$ mol l^{-1}; (d) 90 % acetonitrile, $[C_{70}] = 3.5 \times 10^{-6}$ mol l^{-1}.

the tendency of fullerene molecules to form clusters consisting of some number of molecules. In this case the equilibrium cluster size distribution function depends considerably on both the content and concentration of the solution. Alteration of these parameters changes the thermodynamic characteristics of fullerenes in the solution, so this can provide cluster formation. The electronic spectrum of a cluster consisting of a number of fullerene molecules differs from that of an isolated molecule. In particular, this follows from the above-considered results of measurements of the third-order nonlinear optical susceptibility (see Section 4.1 and Fig. 9). Hence the alteration in the parameters of the solution, stimulating cluster formation, can be drastically reflected in the optical absorption and fluorescent spectra of dissolved molecules. Thus, the mentioned spectra appear to be quite sensitive to both the solution concentration and content of the solvent. This suggests usage of this property of spectra for diagnostics of fullerene solutions.

5. Fractal structures in fullerene solutions

5.1 Measurement of the kinetics of fractal structure growth using the light scattering methods

The tendency of fullerenes in solutions to the aggregation manifests itself in the formation of clusters consisting of a number of fullerene molecules. Therewith, the experimental data show that in parallel with small-sized clusters, which form practically in a moment and contain about ten molecules, in fullerene solutions it is possible the formation of large-sized clusters growing during several months and containing up to several hundreds thousands of molecules. The growth kinetics of large clusters in fullerene solutions was studied experimentally in detail in the set of elegant works [13, 14]. Now we shall consider briefly the methods used in these works and the results obtained. A solution of C_{60} in benzene at concentration around 1g l^{-1}, which is several times lower than the saturated magnitude, was studied at room temperature using static and dynamic light scattering techniques. As a source of light, a 30 mW semiconductor CW diode laser with $\lambda = 790$ nm was used. The radiation scattered at an angle of more than or of the order of 8 deg was monitored with the aid of an optical waveguide detector connected to a photomultiplier. The method of static scattering of light provides the correlation between the magnitude of relative variation of the intensity of radiation scattered at a given angle, due to existence of dissolved matter in the solution, and the average mass of particles of this matter. Therefore, this method provides the determination of the average mass of clusters formed by fullerene molecules in the solution.

The method of dynamic light scattering consists in measuring the spectral line width of scattered radiation due to Brownian motion of particles in the solution. Because the

characteristic velocity of Brownian motion of particles in a solution is inversely proportional to the mean particle radius, this permits the derivation of information on the linear dimensions of dissolved particles. Therefore, by combining the methods of static and dynamic scattering of light, one can both investigate the dynamics of growth of aggregates in a solution and determine the relation between the mass and size of a cluster, i.e. its fractal dimension.

As revealed by the measurements made in Ref. [13], fullerenes in a benzene solution form fractal aggregates with a fractal dimension of about 2.1. The growth of such structures was observed over a period of time up to 100 days. The structures formed are unstable and are destroyed by the light shaking of the solution, after which the formation and growth of fractal structures is restarted. The dynamics of growth of fractal structures is shown in Fig. 13 which gives the measured hydrodynamic radius R_h of fractal clusters as a function of time. It should be noted that the behavior of cluster growth depends to some extent on the manner of preparation of the solution. The data in Fig. 13 correspond to the case when the solution was prepared in the open air with the possibility of access for oxygen. If the solution was prepared in a nitrogen atmosphere without access for oxygen, the measured value of the hydrodynamic radius was approximately 20% higher throughout the entire period of observation.

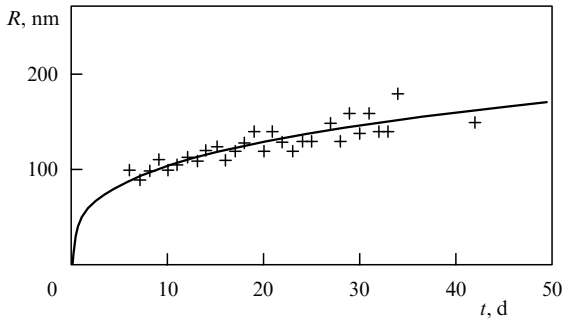

Рис. 13. Dependence on time of growth of the hydrodynamic radius of fractal cluster C_{60} in a benzene solution, measured in Ref. [13]. The solid line is the result of calculations using a modified RLCA model for $D = 2.08$, $\alpha = 2$, and $\gamma_0 = 10^{-7}$.

5.2 The aggregation of particles in solutions. Diffusion approach

As seen from the measurement results, the average radius of the fractal cluster at the end of the observation period reaches a value of ~ 170 nm. This magnitude is in a quite good agreement with the observed data of the above-cited work [50]. In view of the relation between the fractal dimension of a cluster D, its radius R and the number of particles in the cluster n, namely,

$$n = \left(\frac{R}{r_0}\right)^D , \tag{29}$$

where r_0 is the radius of the fullerene molecule, we derive that the maximum number of particles in the cluster, attained during the observation time of $\sim 4 \times 10^6$ s, is approximately 10^5. We shall analyze the kinetics of growth of fractal fullerene clusters in a solution, as observed in Refs [13, 14], on the basis of a simple model approach [51 – 55] traditionally used to describe this process.

Consider an elementary act of coalescence of two particles in a solution under condition (13), when the characteristic value of the Reynolds number for thermal motion of a dissolved molecule is much less than unity. In this case the Brownian motion can be described on the basis of the approach employed by Stokes, Einstein, and Smoluchowski. In accordance with these ideas [51], the rate constant k for the aggregation of particles in a solution is defined by the diffusion mechanism and expressed by the relation

$$k = 4\pi(D_1 + D_2)(r_1 + r_2) . \tag{30}$$

Here r_1 and r_2 are the particle radii, and D_1 and D_2 are their diffusion coefficients in the solution. Using Stokes' formula (12) for the diffusion coefficient of the particles in the solution, we derive the known expression for the rate constant of coalescence of particles [51]:

$$k = \frac{8T}{3\eta} F(r_1, r_2) , \tag{31}$$

where the function

$$F(r_1, r_2) = \frac{(r_1 + r_2)^2}{4 r_1 r_2} \tag{32}$$

is close to unity in the case $r_1 \approx r_2$, and close to $0.25 r_1/r_2$ for $r_1 \gg r_2$. The typical value of saturated concentration of fullerenes in most widely used solvents, corresponding to solubility at room temperature, is $N_0 \sim 10^{18}$ cm^{-3}. The characteristic value of the dynamic viscosity for such solvents is $\eta \sim 0.01$ P. Hence, it follows that the rate constant for coalescence of two fullerene molecules or two clusters of comparable sizes, consisting of these molecules, is $\sim 10^{-12}$ cm^3 s^{-1}, which corresponds to the characteristic time of the attachment process under diffusion approach $\tau \sim (N_0 k)^{-1} \sim 10^{-6}$ s. Apparently, the time required for the establishment of equilibrium size distribution function of small clusters (estimated in the preceding sections) is of the same order.

One can see that the real time of growth of fractal clusters ($\sim 10^6$ s), experimentally obtained in Ref. [13], exceeds the estimation result by many orders of magnitude. Therefore, in describing the kinetics of growth of fractal structures of fullerenes in solutions, one must take into consideration details of the growth mechanism such as the fractal dimension of the structures being formed, the probability of coalescence of approaching clusters (which is less than unity), etc. For this purpose, we shall employ simple models of growth of fractal structures, described in Refs [53 – 55]. These models are based on the assumption of invariability of the fractal dimension of cluster in the process of its growth.

5.3 Models of fractal cluster growth in fullerene solutions

The DLCA model. The simplest model of fractal cluster growth is the diffusion-limited cluster aggregation model (DLCA). In accordance with this model, the aggregation of clusters is a result of attachment of clusters of comparable sizes. The rate constant of this process is determined from relations (30) – (32) and, as follows from the foregoing, is virtually independent of the cluster sizes. In this case, the kinetics of growth of fractal clusters with the average number

of particles n is described by the equation

$$\frac{\mathrm{d}n}{\mathrm{d}t} = N_0 k \,. \tag{33}$$

The right side of Eqn (33) is independent of n, because the concentration of clusters of size n is N_0/n, while the attachment of the cluster of size n to the given cluster results in an increase of its size by n. The rate of cluster growth is proportional to the product of two factors identified above and is equal to $N_0 k$. In view of relation (29), the equation of kinetics of growth of a fractal cluster of average size n within the framework of DLCA model takes the form

$$R = r_0 (N_0 k t)^{1/D} \,. \tag{34}$$

As follows from this expression, the time required to increase the fractal cluster radius by a factor of 500 is of the order of 1 s. It is easy to see that this value differs from the measurement results, given in Fig. 13, by approximately six orders of magnitude. Thus, it should be concluded that the DLCA model does not apply to the experimental conditions of Ref. [13].

The DLA model. Another model used to describe fractal structure growth is also based on the concept of diffusion-limited aggregation (DLA). In accordance with this model, the cluster growth is a result of attachment to given cluster of individual particles such as fullerene molecules or small clusters consisting of these molecules. Assuming that the initial number density N_0 of fullerene molecules in a solution and the average concentration N_c of growing clusters are time-independent, we derive the equation describing the time variation of the average cluster size n:

$$\frac{\mathrm{d}n}{\mathrm{d}t} = (N_0 - nN_\mathrm{c})k \,. \tag{35}$$

Here, in accordance with relations (29)–(32), one has

$$k = n^{1/D} \frac{2T}{3\eta} = k_0 n^{1/D} \,. \tag{36}$$

It should be noted that the form of Eqn (35) is independent of the size of a small cluster attaching to a large cluster of size n. Indeed, let the number of fullerene molecules in a small cluster be equal to n_s, and the concentration of clusters of this size be equal to N_s. Then the rate of growth of large clusters as a result of attachment of small clusters of size n_s is written as

$$\left(\frac{\mathrm{d}n}{\mathrm{d}t}\right)_s = kN_s n_s \,. \tag{37}$$

The summation of this expression over all values $s \ll n$, in view of the obvious normalization condition

$$N_\mathrm{c} n + \sum n_s N_s = N_0 \,, \tag{38}$$

provides equation (33). As a result, it turns out that the growth rate of large fractal clusters does not depend on the shape of the size distribution function of small clusters. This feature is caused by the specific form of the cluster size dependence on the attachment rate constant (32) which, in the limiting case of clusters of highly differing sizes, does not depend on the size of the smaller cluster.

The solution of equation (33) with the initial condition $n(t=0) = 1$ has the following form:

$$t = \frac{1}{k_0 N_\mathrm{c}(1 - 1/D)} \int_1^n \frac{\mathrm{d}n^{1-1/D}}{\bar{n} - n} \,. \tag{39}$$

Here, $\bar{n} = N_0/N_\mathrm{c}$ is the maximum attainable number of particles in a cluster. Expression (39) is considerably simplified in the case $D = 2$:

$$\left(\frac{n}{\bar{n}}\right)^{1/2} = \frac{R}{R_\mathrm{m}} = \frac{\exp(t/\tau\sqrt{\bar{n}}) - 1}{\exp(t/\tau\sqrt{\bar{n}}) + 1} \,, \tag{40}$$

where $R_\mathrm{m} = \sqrt{\bar{n}}\, r_0$ is the maximum attainable cluster radius, and $\tau = (N_0 k_0)^{-1}$. In accordance with the derived expression (40), the characteristic time of cluster growth is of the order of $\tau(\bar{n})^{1/2}$. This conclusion also does not correspond to the experimental data in Fig. 13. Indeed, because the dependence $R(t)$ given in Fig. 13 is close to saturation at the last stage of growth, one may assume for estimation that the value of R_m is close to the maximum measured value 200 nm of the radius. Hence, it follows that $\bar{n} \approx (R_\mathrm{m}/r_0)^2 \approx 3 \times 10^5$, and the characteristic time of cluster growth may be estimated as $\tau(\bar{n})^{1/2} \approx 10^{-3}$ s. Because the measured value of this parameter exceeds the estimation result by nine orders of magnitude, one can conclude that the DLA model is also unsuitable for description of the experimentally examined growth of fractal clusters of fullerenes in a solution.

The RLCA model. Yet another model used to describe the fractal cluster growth is based on the concept of reaction-limited cluster aggregation (RLCA) [53]. In this case, the cluster growth is a result of attachment of clusters of different sizes, with the attachment probability of approaching clusters being $\gamma \ll 1$, so that for a pair of clusters to attach, they must undergo a large number of collisions. The equation describing the kinetics of cluster growth within the RLCA model has the form [51]

$$\frac{\mathrm{d}n}{\mathrm{d}t} = \gamma N_0 \sqrt{\frac{T}{2\pi\mu}} 4\pi (R_1 + R_2)^2 \,, \tag{41}$$

where R_1 and R_2 are the radii of approaching clusters, and μ is their reduced mass. Using relation (29) and averaging equation (41) over the cluster size distribution function, we derive the equation [51]

$$\frac{\mathrm{d}n}{\mathrm{d}t} = J\gamma N_0 \sqrt{\frac{T}{2\pi m_0}} 4\pi r_0^2 n^{2/D - 1/2} \,. \tag{42}$$

Here, r_0 is the radius of the fullerene molecule, and m_0 is its mass. The dimensionless coefficient J depends on the form of the cluster size distribution function, as well as on the cluster fractal dimension D. Thus, $J = 6.8$ for the case of $D = 2$ and the simplest form of this function

$$f \approx \exp\left(-\frac{n}{n_0}\right) , \tag{43}$$

where n_0 is the average number of particles in the cluster. Integration of (42) results in

$$R = r_0 \left[8\pi\gamma N_0 J \left(\frac{3}{2} - \frac{2}{D}\right) \sqrt{\frac{T}{2\pi m_0}} r_0^2 t\right]^{2/(3D-4)} . \tag{44}$$

One can see that the use of the RLCA model leads to an unlimited growth of the cluster radius with time. Because $D \approx 2$, dependence (44) is close to linear. Such a dependence notably differs from the experimental curve shown in Fig. 13. This permits us to conclude that the RLCA model is likewise not applicable to description of the growth of fractal fullerene clusters in a solution.

However, a satisfactory agreement between the calculated and measured evolution of fractal cluster growth can be reached as a result of some modification of the RLCA model. Namely, let us assume that the cluster attachment probability γ depends on the cluster size:

$$\gamma = \gamma_0 \left(\frac{r_0}{R} \right)^{\alpha}. \quad (45)$$

This results in the expression

$$R = r_0 \left[4\pi\gamma_0 N_0 \left(\frac{3}{2} + \frac{\alpha}{2} - \frac{2}{D} \right) \sqrt{\frac{T}{2\pi m_0}} r_0^2 t \right]^{4/(6D+2\alpha D-8)}. \quad (46)$$

Dependence (46) calculated for $D = 2.08$, $\gamma = 2$, and $\gamma_0 = 10^{-7}$ is shown in Fig. 13 by a solid line. This dependence is seen to agree quite well with the experimental data. Notice that the calculated dependence almost coincides with the result of calculation within the simplified model with $D = 2$.

5.4 Small and large clusters in fullerene solutions

As follows from the comparison of the time dependences of the cluster size, calculated within the most widely employed models, with the experimental data, none of these models fits the experiment. The main problem which retards fitting these data consists in the striking difference between the experimentally established characteristic time of cluster growth ($\sim 10^6$ s) and the time estimated on the basis of the Stokes–Einstein–Smoluchowski model. This problem cannot be overcome by introducing the probability of cluster attachment $\gamma \ll 1$ alone, because this leads to unlimited linear growth of the cluster size with time, which is in contrast with the experimental results. A possible way to overcome this problem consists in some modification of the standard RLCA model of fractal cluster growth. Namely, an adequate agreement is reached assuming that the attachment probability for approaching clusters depends on the cluster size. This assumption can be supported with some geometric considerations. In doing so, a large fractal cluster can be treated as a structure with several high and narrow vertices. Then relation (45) with $\alpha = 2$ is valid in the case where the attachment of two large clusters is a result of adherence of two vertices belonging to these clusters.

A more complicated modification of the standard RLCA model may involve abandonment of the commonly made assumption about the time-independence of the fractal dimension of a cluster. As follows from the results of detailed Monte-Carlo calculations [53, 55], the fractal dimension of clusters in the course of their growth tends to increase, which is associated with a gradual filling of large cavities inside the cluster. Accounting for this dependence could help to eliminate the discrepancy between the theoretical and experimental data. However, more detailed experimental investigations are required in order to reliably determine the form of this dependence.

The analysis of experimental data concerning peculiarities of the formation and growth of fullerene clusters in solutions generates one more problem relating to a considerable difference in the size of clusters, observed in different experiments. So, the experiments directed to the measurement of the temperature dependence of the solubility of C_{60} in hexane, toluene and CS_2 [7] as well as the concentration dependence of the third-order nonlinear optical susceptibility of C_{60} dissolved in benzene [8] are followed by the conclusion of the existence in these solutions of clusters consisting of about 10–20 fullerene molecules. This conclusion is also supported by the results of direct measurements performed using the photoluminescence spectroscopy method [50], in accordance with which the fullerene molecules C_{60} dissolved in benzene, toluene and CS_2 form aggregates of several nanometers in size. On the other hand, the optical experiments [13, 14] performed using the static and dynamic light scattering methods show a possibility of formation in fullerene solutions of much larger clusters consisting of more than a hundred thousand molecules per cluster and measuring several hundreds of nanometers in size. Thus, as was stated in works [13, 14], the clusters have a fractal structure with fractal dimension ~ 2.1, and the process of growth takes tens of days.

The contradiction noted between the results of different experiments can be eliminated taking into consideration the bimodal form of the cluster size distribution (see Fig. 12), observed in work [50]. Apparently, small-sized clusters are formed in a short time, which can be estimated through the relation $\tau \sim (N_0 k)^{-1} \sim 10^{-6}$ s, where N_0 is the concentration of fullerenes in a solution and the attachment rate constant k is given by formula (31). This is a crude estimate for the time necessary for establishing the quasi-equilibrium cluster size distribution function, which can be found qualitatively on the basis of the droplet model of a cluster [see equations (4), (8)]. Larger-sized clusters having a fractal structure are formed as a result of much slower aggregation processes, the characteristic time of which at the initial stage of growth measures tens of seconds, and at a later time rises proportionally to the squared cluster diameter. As follows from the direct observation results, such structures are destroyed quite easily under hand shaking of a solution. It follows that the binding energy of these fractal structures is relatively low. Thus it is explained an apparent contradiction between the results of different experiments, used for estimation of the cluster size.

6. Thermodynamic parameters of fullerite

6.1 Close-packed crystals and short-range intermolecular interaction

The behavior of fullerenes in solutions essentially depends on the thermodynamic properties of this substance in the solid phase. Indeed, the main parameter characterizing the behavior of fullerenes in solution is solubility. In accordance with the results of analysis performed in Section 2 of the article [see equations (3), (4)], the solubility of fullerene as well as any other phase equilibrium state is expressed through the difference between the chemical potential of a molecule positioned in a solution and the solid phase, respectively. Thus, it turns out that a change in the crystal structure of fullerene, which is in equilibrium with solution, is reflected on properties of the solution.

Below is presented an approach to the establishment of thermodynamic properties of fullerite (i.e. the crystal produced from fullerene molecules) based on similarity laws for crystal structures consisting of close-packed particles with a short-range interaction [56–58]. Here, the term 'short-range interaction' means a pair interatomic (intermolecular) interaction between particles in the crystal, acting over the limited range of the interparticle distances. For condensed media this means a prevailing role of the pairwise interaction between neighboring particles. The parameters of this interaction

determine the main thermodynamic characteristics of the system. Such structures make up a special class of substances, whose thermodynamic parameters are characterized by common peculiarities [56, 57]. Along with rare gas crystals, to this class of structures also belongs crystal fullerite at a temperature exceeding the point of phase transition (260 K) accompanied with disordering of the molecular orientation and defreezing of molecular rotation [34, 35].

As a typical example of the systems discussed the rare gases (excluding helium) can be considered, whose crystal structure is face-centered cubic (fcc) with close-packed atoms. As shown in Refs [56, 57], all the thermodynamic parameters of those systems being expressed in a dimensionless form coincide very closely. The reason is the low sensitivity of thermodynamic characteristics to small differences in the form of the potential $V(R)$ for atoms of various kinds. Thus, to determine the main thermodynamic characteristics of a substance with experimental accuracy, the only two parameters related to the potential energy curve are sufficient to know: the well depth D and equilibrium distance R_0. These parameters determine in a natural manner the set of dimensionless variables which in turn generates the similarity of thermodynamic functions. Thus, the temperature dependence of the saturated vapor pressure $p(T)$ for all rare gases is expressed in a unified form [57] as

$$\frac{p}{p_0} = \phi\left(\frac{T}{D}\right). \tag{47}$$

Here $p_0 = D/R_0^2$ is the natural unit of pressure for the systems under consideration. As the natural unit of density for such systems the expression $\rho_0 = \mu/R_0^3$ could be used, where μ is the atomic mass. In so doing, the critical parameters of a system are expressed in a unified manner through the inherent natural units:

$$p_c = (0.131 \pm 0.001)p_0\,, \tag{48}$$

$$\rho_c = (0.301 \pm 0.001)\rho_0\,, \tag{49}$$

$$T_c = (1.04 \pm 0.02)D\,. \tag{50}$$

The numerical factors in equations (48)–(50) were obtained as a result of a statistical averaging of the experimental data for rare gases [57]. Other thermodynamic parameters of rare gases, such as the melting and boiling points T_m and T_b, the densities of crystal ρ_s and liquid ρ_l at those temperatures as well as the bulk modulus, volume and linear thermal expansion coefficients, etc., are determined in a similar way through the natural units of the system. Taking into account Eqns (48)–(50), relation (47) can be expressed as follows

$$\frac{p}{p_c} = f\left(\frac{T_c}{T}\right); \tag{51}$$

this relation is universal as given above.

Attention should be drawn to the fact that fullerenes discovered in the solid state (fullerites) may also be related to the considered class of systems of spherically symmetrical close-packed and short-range interacting particles. The similarity in crystal structures of solid fullerenes and rare gas crystals provides a way of reliably estimating the thermodynamic quantities of fullerenes. These estimates fit quite well the experimental data, when they exist. The comparison of these estimates with results of recent numerical calculations and with estimated parameters of intermolecular interaction potential obtained on the base of measurements of saturated vapor pressure, permits a refinement of the magnitudes of those parameters and also a determination of the degree of sensitivity of thermodynamic characteristics of fullerenes to details in the intermolecular interaction potential.

6.2 Binding energy of fullerenes in crystals

Let us consider the crystalline state of fullerene C_{60} at temperatures exceeding the critical point (260 K) for an orientational disorder phase transition, which is accompanied by defreezing the free thermal rotation of C_{60} molecules in the fullerite crystal about their axes [34, 35]. In these conditions the fullerene molecules forming the crystal can be considered as spherically symmetric systems with a pair intermolecular interaction potential. The characteristic binding energy of carbon atoms in a fullerene molecule is much more than that of fullerene molecules in crystal. The main thermodynamic behavior of this crystal is determined by the parameters of that potential, namely, the well depth D and the equilibrium distance between the centers of molecules R_0. In systems with short-range interaction and face-centered cubic structure, the parameter R_0 determines the distance between the nearest neighbors in a crystal. The parameters of the crystal structure of fullerenes are stated quite well. Thus, for fullerene C_{60} crystal at $T = 260$ K, the quantity $R_0 = 1.006$ nm [5, 59], which provides the crystal density $\rho = 1.69\ \mathrm{g\,cm^{-3}}$. As for the parameter D, its value is known with a considerable uncertainty. In Table 5, the values of this parameter determined in various calculations and experiments are shown. Here, the data for $T = 0$ were obtained through the summation of all van der Waals interaction potentials between atoms belonging to two neighboring C_{60} molecules. The statistical averaging of the data presented results in $D = (0.306 \pm 0.044)$ eV.

As is seen, the values of the parameter D obtained on the base of independent measurements and calculations are characterized by a considerable statistical spread. This hinders the use of this parameter for quantitative estimation of thermodynamic quantities of fullerite. One of the main reasons of this data spread is in the most useful way for estimating the parameter D, based on fitting the measured temperature dependences of saturated vapor through the Arrhenius equation. Since such measurements are usually performed in a limited temperature range, whereas the true temperature dependence $p(T)$ can differ notably from the

Table 5. Binding energy of two fullerene C_{60} molecules measured and calculated by various authors.

T, K	298	700	773	788	600	0	0	780	770	0
D, eV	0.4	0.32	0.275	0.290	0.240	0.32	0.275	0.31	0.347	0.288
References	[60]	[61]	[62]	[63]	[64]	[65]	[66]	[67]	[68]	[69]

Arrhenius exponent, the measurement data obtained in different temperature ranges can differ considerably from one another.

6.3 Saturated vapor pressure

A more accurate estimation of the quantity D and other parameters characterizing the thermodynamic properties of fullerite can be obtained using the similarity relations (47)–(51). In doing so, it appears to be appropriate to use the above-noted similarity of corresponding dependences for close-packed systems with the short-range interaction. The measured temperature dependences of the saturated vapor pressure for fullerene molecules C_{60} have to be expressed in a dimensionless form (51). The value of the parameter D involved into this dependence will be determined by fitting the function $p(T_c/T)$ for fullerene with the corresponding function for rare gases.

The saturated vapor pressure for rare gases has been measured in various works. The experimental data are reviewed particularly in Ref. [56]. The dependences of reduced saturated vapor p/p_c on T_c/T, determined for Ne, Ar, Kr, and Xe on the base of these data, are shown in Fig. 14. The fulfillment of the similarity law (51), which is sometimes called the law of corresponding states, can be seen. Some deviation of data for Ne in the low-temperature region is caused by well-known quantum effects. The dependence $p(T)$ has a characteristic bend at the triple point.

The same figure shows the measured and calculated data for the saturated vapor pressure of C_{60} fullerene [61–64, 67, 68], processed in accordance with the similarity law (51) considering relations (47)–(50). The values of critical temperature and pressure for fullerene were calculated using Eqns (48), (50) for a fixed D value. Notice that both values are proportional to D. The broken lines in Fig. 14 correspond to the extreme D values from Table 5 ($D = 0.24$ eV and $D = 0.35$ eV). As can be seen, the dependences $p(T)$ obtained with these values do not agree with the similarity law (51) for inert gases. The best fitting of dimensionless temperature dependences of saturated vapor pressure for fullerene with those for rare gases is reached for $D = 0.257$ eV. This value lies in the range of magnitudes of D obtained in Refs [61–64, 67, 68] and somewhat lower than the result of averaging them (0.306 eV). The temperature dependence of saturated vapor pressure for fullerene, determined using this value of D, is shown in Fig. 14 by asterisks. As is seen, this dependence $p(T)$ agrees quite well with the universal dependence for rare gases. In accordance with Ref. [56], the error in measuring the pressure in the temperature range under consideration does not exceed 5%. One would expect that the above-determined value of D is characterized by an error of the same order of magnitude. Thus, the range of allowable values of D can be stated as 0.257 ± 0.013 eV that is essentially narrower than the above-given error interval evaluated from statistical averaging of the findings of numerous researchers.

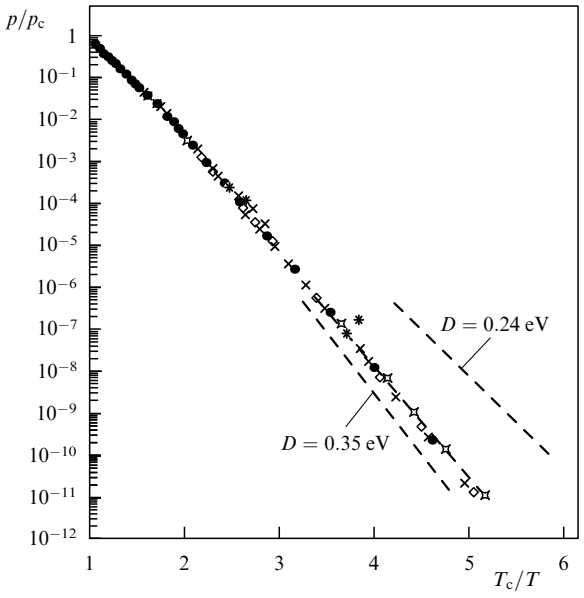

Рис. 14. Dependence on temperature of the saturated vapor pressure in the introduced coordinates: *, •, ◇, × — experimental data [69]; - - - — calculations in Ref. [58] for $D = 0.24$ and 0.35 eV; ☆ — dependence (51) calculated for fullerenes given $D = 0.257$ eV.

6.4 Thermodynamic parameters of fullerite

Assuming fulfillment of the similarity laws (47)–(49) and using the value $D = 0.257$ eV stated above, we obtain the set of critical parameters for fullerene C_{60}:

$$T_c = 3100 \text{ K}, \quad p_c = 53.6 \text{ atm}, \quad \rho_c = 0.5 \text{ g cm}^{-3}. \quad (52)$$

Let us use the critical parameters determined above for checking the fulfillment of the similarity laws for other thermodynamic parameters of fullerite. The first is the compressibility factor at the critical point

$$Z_c = \frac{\mu p_c}{R T_c \rho_c}, \quad (53)$$

where μ is the molecular mass, and R is the universal gas constant. The values of Z_c for rare gases and fullerene C_{60} are shown in Table 6. Some other fullerite parameters are also presented. Thus, the dimensionless heat of evaporation q at $T = 0$ K is determined as follows

$$q = \frac{q_0 \rho_c}{p_c}, \quad (54)$$

where q_0 is the specific heat of evaporation at $T = 0$. In Table 6, data related to the isothermal compressibility modulus K_T are also presented. These quantities for rare gases were taken from Ref. [70], and for C_{60} from Ref. [71]. It is easy to show that the similarity laws (47)–(51) cause the ratio K_T/p_c to be constant. The values of this ratio are also given in Table 6. The fulfillment of the similarity law for these values is somewhat poor in comparison with other ones. Apparently it is caused by the limited accuracy of their measurements.

Let us determine the similarity relation for the Debye temperature. In its physical sense the energy corresponding to the Debye temperature is proportional to the characteristic energy of vibration $\hbar\omega$ of the crystal lattice. From the parameters D, R_0 and μ only a quantity with the dimension of frequency can be constructed:

$$\omega_D \sim \frac{(D/\mu)^{1/2}}{R_0}. \quad (55)$$

The Debye temperature has to be proportional to this frequency, which is an inherent natural unit for it. Thus, the dimensionless Debye temperature is defined by the ratio

$$\theta_0 = \frac{\omega_D R_0}{(D/\mu)^{1/2}}. \quad (56)$$

Table 6. Thermodynamic parameters for rare-gas and fullerite C_{60} crystals.

Parameter	Ne	Ar	Kr	Xe	C_{60}
D, meV	3.7	12.2	17.2	24	257
R_0, nm	0.307	0.376	0.401	0.436	1.006
μ, u	20.2	39.9	83.7	131.3	720
T_c, K	44.4	150.7	209.4	289.7	3100
p_c, bar	26.5	48.6	55.2	58.4	53.6
ρ_c, g cm^{-3}	0.484	0.535	0.919	1.11	0.5
ω_D, K	75	92	72	64	74
q_0, J g^{-1}	93.3	193.7	133.8	126	230
K_T, kbar	11	28.6	34.4	36.5	18
Z_c	0.302	0.292	0.288	0.287	0.30
q	17.0	21.1	22.2	22.9	21.4
K_T/p_c	415	586	624	625	335
θ_0	22.7	26.4	26.9	27.5	52.6

In accordance with the similarity laws, the values of this dimensionless parameter for all crystals belonging to the considered class should be close. The values of θ_0 in Table 6 are determined through relation (56) from experimental and estimated data. As can be seen, similarity relation (56) is fulfilled quite well for the rare-gas crystals. Some (of the order of 15%) violation of this relation for Ne is attributed to well-known quantum effects at low temperatures. The value of ω_D for fullerite was taken from Ref. [71]. The value of θ_0 for fullerite is about twice as high as that for rare-gas crystals. Such a deviation of the fullerite Debye temperature from the value followed from similarity relation (56) does not appear to be surprising, since over a temperature range near the Debye point (74 K) the fullerite crystal is orientally ordered, so that its structure is dissimilar to face-centered cubic. Thus, a fullerene molecule whose thermal rotation is frozen cannot be considered as a spherically symmetric particle. Therefore the fulfillment of the similarity laws which are valuable for particles with spherically symmetric interaction potential would hardly be expected. Further, some contribution to the Debye spectrum of fullerite is made by intramolecular vibrations, which of course are not considered in fomulating the similarity laws. If the intramolecular and intermolecular vibration frequencies in the Debye temperature range are of the same order, this should be reflected in the value of Debye frequency. Thus, this conclusion depends on the degree of plausibility of the Debye temperature measured in Ref. [71]. Notice that in order for similarity law (56) to be met, the fullerite Debye temperature has to be set at $\omega_D = 40$ K.

6.5 The problem of the existence of liquid fullerite

Therefore, the above-presented comparison of results of independent measurements and calculations shows that the similarity relations can be used for estimating the magnitudes of a large number of physical parameters of fullerite. In so doing, the estimation error as a rule does not exceed the corresponding value for rare-gas crystals. The sole exception is the Debye temperature for fullerite, measured in Ref. [71]. This disagreement is caused by freezing the fullerene molecules' rotation in crystals at low temperatures, which provides the dissimilarity between the real intermolecular interaction potential and the spherically symmetric one.

The estimates performed permit light to be shed on a question of basic importance, which is the subject of lively discussion in contemporary publications [72 – 74]. The question is whether fullerene can exist in a liquid state? Various calculations performed using the model intermolecular interaction potential [66] give both positive [73, 74] and negative [72] answers to this question. The negative answer obtained in Ref. [72] is explained by the prominent difference of the intermolecular interaction potential [66] from the Lenard – Jones one. An insignificant deviation of the main thermodynamic parameters of fullerene from the corresponding magnitudes of those determined through the similarity laws shows a weak sensitivity of the values of those parameters to the specific form of the intermolecular interaction potential. This permits one to expect that fullerite just as other systems of close-packed spherically symmetric molecules with a short-range interaction can exist in a liquid state in some temperature region. At atmospheric pressure, this rather narrow region ranges from the melting point $T_m = 0.58$ $D = 1729$ K up to the boiling point $T_b = 0.61$ $D = 1820$ K. The only obstacle to this can be the thermal decomposition of fullerene molecules in this temperature range. However, calculations [75] and experiments [76] performed recently show a high thermal stability of fullerenes at atmospheric pressure at least up to 2000 K. There is a reason to believe that the above-formulated approach will stimulate further studies directed to the extension of our knowledge about the thermodynamic properties of fullerenes in various phase states.

7. Conclusions

Fullerenes are a unique object of chemical physics, whose behavior in many physical situations is characterized by remarkable peculiarities. Peculiarities in the behavior of fullerenes in solutions show up firstly in that fullerenes represent the only soluble form of carbon. This is related primary to the originality in the molecular structure of fullerenes. The fullerene molecule is a virtually uniform closed spherical or spheroidal surface having no sharp ridges or dents. Such a structure gives rise to the relatively weak interaction between the neighboring molecules in a fullerite crystal and promotes effective interaction of the molecules with those of a solvent.

Another interesting peculiarity of the behavior of fullerenes in solutions is related to their tendency to form clusters consisting of a number of fullerene molecules. The energy of interaction of a fullerene molecule with solvent molecules is proportional to the surface of the former molecule and roughly independent of the relative orientation of solvent molecules. The value of this energy accounted per fullerene

molecule is somewhat lower than the binding energy of neighboring molecules in a fullerite crystal at $T > 260$ K (phase transition point). This promotes formation of extended fractal structures in the solution with predominance of the surface energy of interaction between fullerene molecules and solvent over the volume energy of interaction between neighboring fullerene molecules. Notice that a direct indication of the tendency of diluted fullerenes to aggregation was found in one of the early studies [77], where the evaporation of solvent (benzene) from C_{60} solution resulted in formation of globules with a mean diameter of the order of 1.5 nm. One can readily estimate that the average number of fullerene molecules in such a globule is about ten.

The analysis performed in the article of experiments concerning the behavior of fullerenes in solutions shows that over a wide range of conditions fullerenes in solutions exist in the form of aggregates or clusters containing from ten up to tens of thousands of particles. Therefore, fullerenes in solutions represent a unique case of a 'cluster' substance, the thermodynamically equilibrium state of which corresponds to the majority of the matter in the cluster form. Such a unique peculiarity, attributed to details in the interaction of fullerene molecules with one another and with solvent molecules, can be realized only in solutions, whereas the 'cluster' substance in the gas phase can be produced only in highly nonequilibrium conditions [78], for example, in the conditions of a supersonic nozzle. This peculiarity makes fullerenes in solutions an interesting object from the viewpoint of the investigation of the properties of a 'cluster' substance.

The aggregation of fullerenes is reflected in various physical and chemical properties of fullerene solutions. Thus, this phenomenon causes the extraordinary (decreasing) temperature dependence of solubility and unusual concentration and temperature dependences of optical parameters and transport coefficients of fullerenes in solutions. As a result of aggregation in fullerene solutions ensue the solvatochromism phenomena showing up in a sharp dependence of the optical absorption spectra of solutions on their concentration and the content of the solvent.

All these phenomena were observed in experiments and have a unified explanation in the framework of the droplet model of a cluster, in accordance with which the free energy of a fullerene molecule involved in a cluster is combined from two components: a volume one, which is proportional to the number of molecules n in a cluster, and a surface one, which is proportional to $n^{2/3}$. Further development of this approach to the description of peculiarities in the behavior of fullerenes in solutions should lead to consideration of the behavior of fullerenes in composite solutions consisting a mixture of various solvents. This will permit us to obtain the comprehensive description of solvatochromism phenomenon as a result of varying the cluster size distribution function caused by a change in the content of a solvent.

The tendency of fullerenes to form clusters in solutions must be taken into consideration when further developing the technology of enrichment, separation, and purification of fullerenes. This applies in particular to the problem of preparation of higher fullerenes in macroscopic amounts, which still awaits a process solution. The main difficulty in solving this problem lies in the exceedingly low content of higher fullerenes in fullerene-containing soot which is formed as a result of thermal deposition of graphite. In this regard the problem appears similar to that of enrichment and separation of isotopes. One of the possible ways of solving this problem may be based on the concentration dependences of the diffusion and thermal diffusion coefficients of fullerenes in solutions, established in this study. The attainable values of the separation factor prove much higher than the respective values that are at the basis of the existing efficient technologies of isotope enrichment and separation. And, because the market value of higher fullerenes is highly competitive with that of many stable isotopes, the efforts aimed at developing relevant technologies appear economically justified. It is hoped that this review paper will both aid to expand our basic knowledge of the behavior of fullerenes in solutions and stimulate such efforts.

The authors are indebted to B M Smirnov for his interest in the work, and to RFBR for partial support (Grant No. 96-02-160008a).

References

1. Kroto H W et al. *Nature* (London) **318** 162 (1985); see also Kroto H W "Nobel lectures on chemistry — 1996" *Usp. Fiz. Nauk* **168** (3) 343 – 358 (1998)
2. Krätschmer W et al. *Nature* (London) **347** 354 (1990)
3. Taylor R et al. *J. Chem. Soc. Chem. Commun.* 1423 (1990)
4. Haufler R E et al. *J. Phys. Chem.* **94** 8634 (1990)
5. Eletskiĭ A V, Smirnov B M *Usp. Fiz. Nauk* **163** (2) 33 (1993) [*Phys. Usp.* **36** 202 (1993)]
6. Eletskiĭ A V, Smirnov B M *Usp. Fiz. Nauk* **165** 977 (1995) [*Phys. Usp.* **38** 935 (1995)]
7. Ruoff R S, Malhotra R, Huestis D L *Nature* (London) **361** 140 (1993)
8. Blau W J et al. *Phys. Rev. Lett.* **67** 1423 (1991)
9. Sun Y-P, Bunker C E *Nature* (London) **365** 398 (1993)
10. Hirendra N et al. *J. Phys. Chem.* **100** 9439 (1996)
11. Bezmelnitsyn V N, Eletskii A V, Stepanov E V, in *Progress in Fullerene Research* (Eds H Kuzmany et al.) (Singapore: World Scientific, 1994) p. 45
12. Bezmelnitsyn V N, Eletskii A V, Stepanov E V *J. Phys. Chem.* **98** 6665 (1994)
13. Ying Q, Marecek J, Chu B *Chem. Phys. Lett.* **219** 214 (1994)
14. Ying Q, Marecek J, Chu B *J. Chem. Phys.* **101** 2665 (1994)
15. Suzuki K et al., in *Molecular Nanostructures* (Eds H Kuzmany et al.) (Singapore: World Scientific, 1998)
16. Bezmel'nitsyn V N, Eletskiĭ A V, Stepanov E V *Zh. Fiz. Khim.* **69** 735 (1995)
17. Diederich F et al. *Science* **254** 1768 (1992)
18. Fleming R M et al. *MRS Symp. Proc.* **206** 691 (1991)
19. Meng R L et al. *Appl. Phys. Lett.* **59** 3402 (1991)
20. Eletskiĭ A V *Teplofiz. Vys. Temp.* **34** 308 (1996)
21. Mihaly T, Mandi G *Fullerene Sci. Technol.* **5** (2) 291 (1997)
22. Ruoff R S et al. *J. Phys. Chem.* **97** 3379 (1993)
23. Sivaraman N et al. *J. Org. Chem.* **57** 6007 (1992)
24. Beck M T, Mandi G, Keki S *Fullerene Sci. Technol.* **2** 1510 (1995)
25. Beck M T, Mandi G *Fullerene Sci. Technol.* **3** 32 (1996)
26. Sivaraman N et al., in *185th Meet. Electrochemical Society of America,* May 1994, San Francisco, Rep. 1211
27. Scrivenns W A, Tour J M *J. Chem. Soc. Chem. Commun.* 1207 (1993)
28. Beck M T, Mandi G *Fullerene Sci. Technol.* **5** (2) 291 (1996)
29. Zhou X et al. *Fullerene Sci. Technol.* **5** (1) 285 (1997)
30. Letcher T M et al. *S.-Afr. J. Chem.* **46** 41 (1993)
31. Heyman D *Fullerene Sci. Technol.* **4** 509 (1996)
32. Frenkel' Ya I *Kineticheskaya Teoriya Zhidkosteĭ* (Kinetic Theory of Liquids) (Leningrad: Nauka, 1975) [Translated into English (Oxford: Oxford University Press, 1946)]
33. Smirnov B M *Usp. Fiz. Nauk* **162** (1) 119 (1992); **163** (10) 29 (1993) [*Sov. Phys. Usp.* **35** 37 (1992); *Phys. Usp.* **36** 933 (1993)]
34. Heiney P A et al. *Phys. Rev. Lett.* **66** 2911 (1991)
35. David W I F et al. *Europhys. Lett.* **18** 219 (1992)
36. Honeychuck R V, Cruger T W, Milliken J *J. Am. Chem. Soc.* **115** 3034 (1993)
37. Bezmel'nitsyn V N et al. *Khim. Fiz.* **13** (12) 156 (1994)

38. Smith A L, Walter E, in *Proc. 2nd Symp. Recent Advances in the Chemistry and Physics of Fullerenes and Related Materials, 1995, Reno, Nevada* (Proc. Electrochemical Society, Vol. 95–10, Eds R S Ruoff, K M Kadish) (Pennington, NJ: Electrochemical Soc., 1995) p. 1552
39. Sivaraman N et al., in *Proc. Symp. Recent Advances in the Chemistry and Physics of Fullerenes and Related Materials* (Proc. Electrochemical Society, Vol. 94–24, Eds K M Kadish, R S Ruoff) (Pennington, NJ: Electrochemical Society, 1994) p. 443
40. Smith A L et al., in *Proc. Symp. Recent Advances in the Chemistry and Physics of Fullerenes and Related Materials* (Proc. Electrochemical Society, Vol. 94–24, Eds K M Kadish, R S Ruoff) (Pennington, NJ: Electrochemical Society, 1994) p. 156
41. Dubois D et al. *J. Phys. Chem.* **96** 7137 (1992)
42. Hasemeyer R et al. *Ber. Bunsenges. Phys. Chem.* **98** 878 (1994)
43. Kato T, Kikuchi K, Achiba Y *J. Phys. Chem.* **97** 10251 (1993)
44. Bezmelnitsyn V N et al. *Phys. Scripta* **53** 364 (1996)
45. Shpol'skiĭ È V *Atomnaya Fizika* Tom 1 (Atomic Physics. Vol. 1) (Moscow: Fizmatgiz, 1984) [Translated into English (London: Iliffe Books, 1969)]
46. Andreev B M, Zel'venskiĭ, Ya D, Katal'nikov S G *Razdelenie Stabil'nykh Izotopov Fiziko-Khimicheskimi Metodami* (Separation of Stable Isotopes by Physicochemical Methods) (Moscow: Energoatomizdat, 1982)
47. Bezmel'nitsyn V N et al. *Zh. Tech. Fiz.* **66** (10) 26 (1996) [*Tech. Phys.* **41** 986 (1996)]
48. Bezmel'nitsyn V N et al. *Phys. Scripta* **53** 368 (1996)
49. Bezmel'nitsyn V N, Eletskiĭ A V, Okun' M V *Khim. Fiz.* **17** 140 (1998)
50. Ghosh H N, Sapre A V, Mittal J P *J. Phys. Chem.* **100** 9439 (1996)
51. Eletskii A V, Okun M V, Smirnov B M *Phys. Scripta* **55** 363 (1997)
52. Eletskii A V, Okun M V, Smirnov B M, in *Proc. 2nd Symp. Recent Advances in the Chemistry and Physics of Fullerenes and Related Materials, 1995, Reno, Nevada* (Proc. Electrochemical Society, Vol. 95–10, Eds R S Ruoff, K M Kadish) (Pennington, NJ: Electrochemical Society, 1995) p. 1612
53. Smirnov B M *Fizika Fraktal'nykh Klasterov* (The Physics of Fractal Clusters) (Moscow: Nauka, 1991)
54. Jullien R, Botet R *Aggregation and Fractal Aggregates* (Singapore: World Scientific, 1987)
55. Vicsek T *Fractal Growth Phenomena* (Singapore: World Scientific, 1989)
56. Crawford R K, in *Rare Gas Solids 2* Vol. 2 (Eds M L Klein, J A Venables) (New York: Academic Press, 1997) p. 663
57. Smirnov B M *Usp. Fiz. Nauk* **162** (12) 97 (1992) [*Sov. Phys. Usp.* **35** 1052 (1992)]
58. Vorob'ev V S, Eletskiĭ A V *Teplofiz. Vys. Temp.* **33** 862 (1995) [*High Temperatures* **33** 858 (1995)]; Vorob'ev V S, Eletskii A V *Chem. Phys. Lett.* **254** 263 (1996)
59. Eletskiĭ A V, Smirnov B M *Usp. Fiz. Nauk* **161** (7) 173 (1991) [*Sov. Phys. Usp.* **34** 616 (1991)]
60. Anderson H et al., in *Progress in Fullerene Research* (Eds H Kuzmany et al.) (Singapore: World Scientific, 1994) p. 13
61. Mathews C K et al. *J. Phys. Chem.* **96** 3566 (1992); **98** 1333 (1994)
62. Abrefah J et al. *Appl. Phys. Lett.* **60** 1313 (1992)
63. Chen H S et al. *J. Phys. Chem.* **96** 1016 (1992)
64. Tokmakov A, Haynes A, George S M *Chem. Phys. Lett.* **186** 450 (1991)
65. Ju J et al. *Phys. Rev. B* **49** 5008 (1994)
66. Girifalco L A *J. Phys. Chem.* **95** 5370 (1991); **96** 858 (1992)
67. Korobov M V, Sidorov L N *Zh. Khim. Termodin.* **26** 61 (1994)
68. Richter H et al. *Ber. Bunsenges. Phys. Chem.* **98** 1329 (1994)
69. Girard Ch. et al. *Phys. Rev. B* **49** 11425 (1994)
70. Swenson C A, in *Rare Gas Solids* Vol. 2 (Eds M L Klein, J A Venables) (London: Academic Press, 1977) p. 743
71. Hebard A F *Ann. Rev. Mater. Sci.* **23** 159 (1993)
72. Hagen M H J et al. *Nature* (London) **365** 425 (1993)
73. Ashcroft N W *Nature* (London) **365** 387 (1993)
74. Cheng A, Klein M L, Caccamo C *Phys. Rev. Lett.* **71** 1200 (1993)
75. Zhang B L et al. *Z. Phys. D* **26** 285 (1993)
76. Kolodney E, Tsipinyuk B, Budrevich A *J. Chem. Phys.* **100** 8542 (1994)
77. Wragg J L et al. *Nature* (London) **348** 623 (1990)
78. Smirnov B M *Usp. Fiz. Nauk* **167** 1169 (1997) [*Phys. Usp.* **40** 1117 (1997)]